OSAKA UNIVERSITY

Mathematics for *Advancing* Cardiovascular Medicine

From Hemodynamic Analysis to Clinical Application

AOWM - IPMU Workshop

March 6, 2026 Kavli IPMU

Math × Med

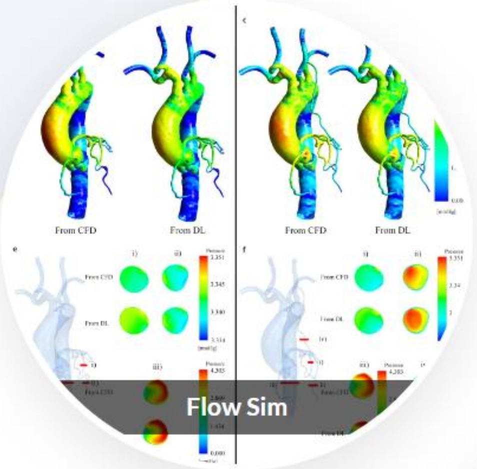

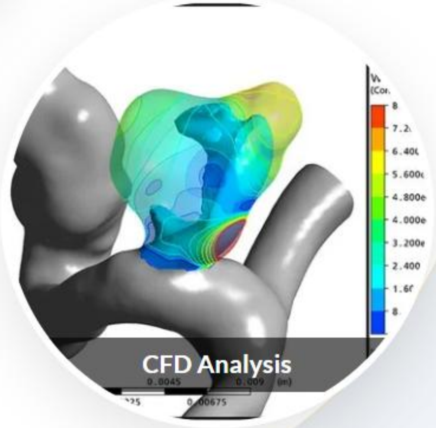

$\nabla \cdot v = 0$

SPEAKER

Yoshie Sugiyama

Professor, Department of Applied Analysis

Osaka University Graduate School of Information Science and Technology

HEMODYNAMICS CFD ANALYSIS AI INTEGRATION

Mathematics × Medicine: Research Journey

> "As a mathematician, I have been engaged in interdisciplinary research. My work bridges mathematics and medicine to support better healthcare."

2015 2019 2020 2026

2015 - 2019

PRESTO

JST PRESTO

Chemotaxis Dynamics of Leukocytes: Research and Application into an Individualized (Tailored) Treatment of Cancer

2020 - 2026 (Current)

CREST

JST CREST

Fusion of Mathematical Analysis and AI Technology Using the Wall Micromotion Based on Medical Images of 4D-CTA / 4D-MRA — Mathematical Data Science Integrated Simulation for Preemptive Medicine

Area: Creation of Core Technology for Solving Social Issues through Integration of Mathematics and Information Science

interdisciplinary research

Mathematics × Medicine × Information Science

Challenge 30,000–250,000 analysis points

time-evolving point cloud data

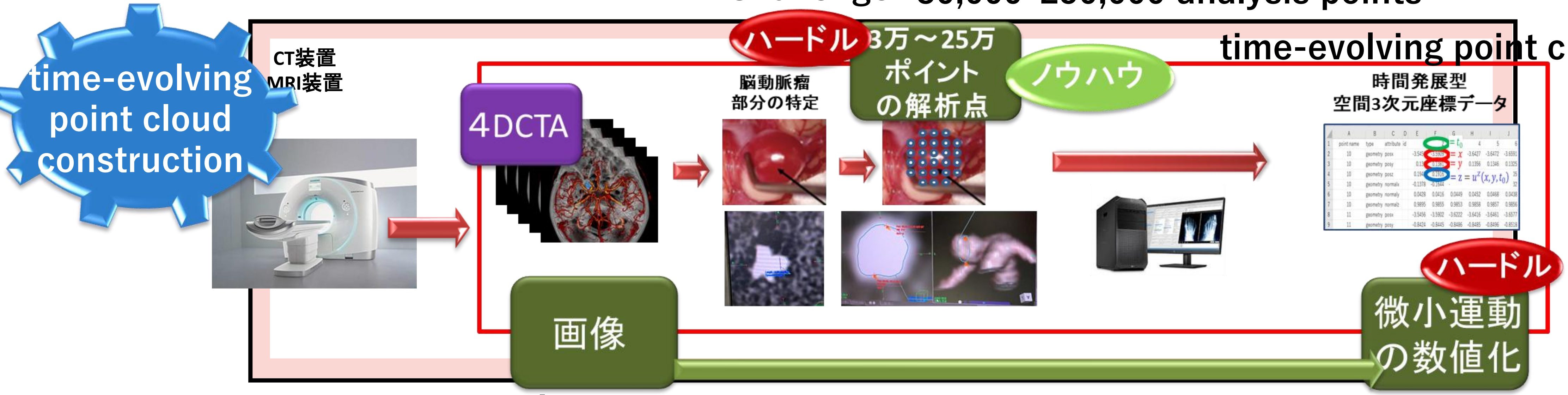

Challenge

Images

Quantification of micro-motion

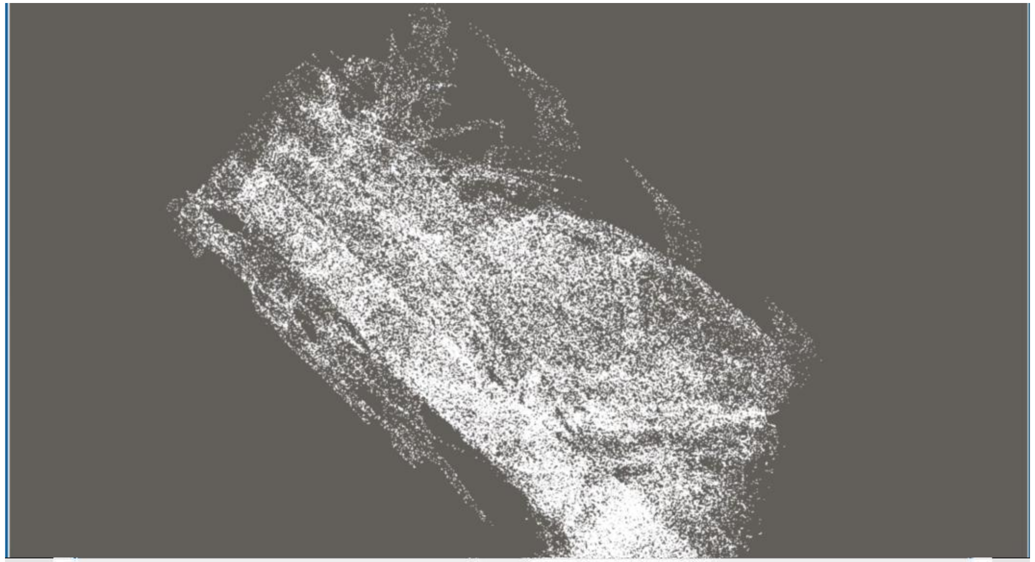

CT輝度値追従 (Intensity-based Tracking)

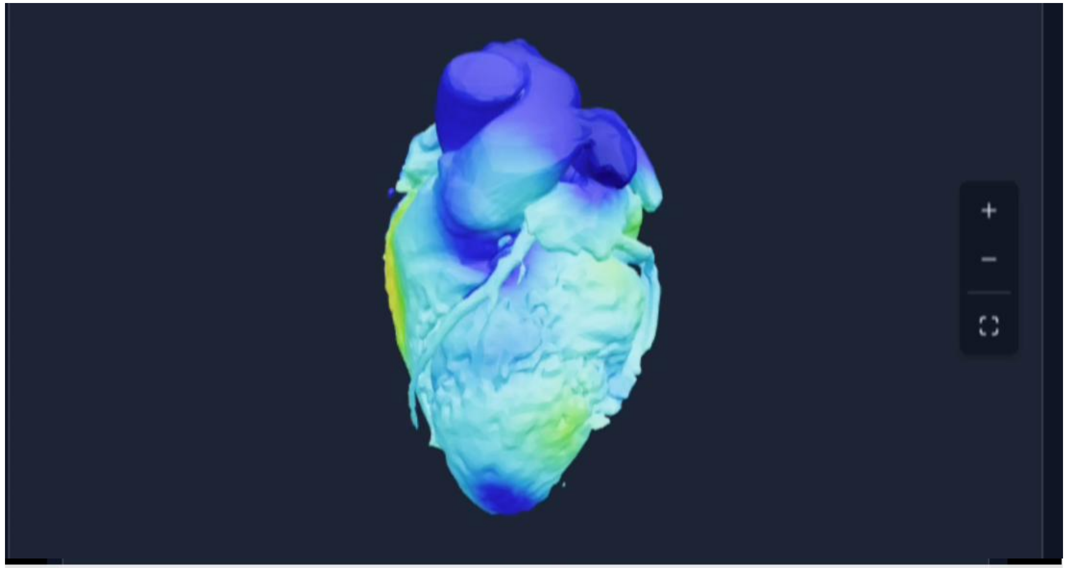

時間方向追従結果 (Temporal Tracking Results)

interdisciplinary research

Mathematics × Medicine × Information Science

time-evolving point cloud construction

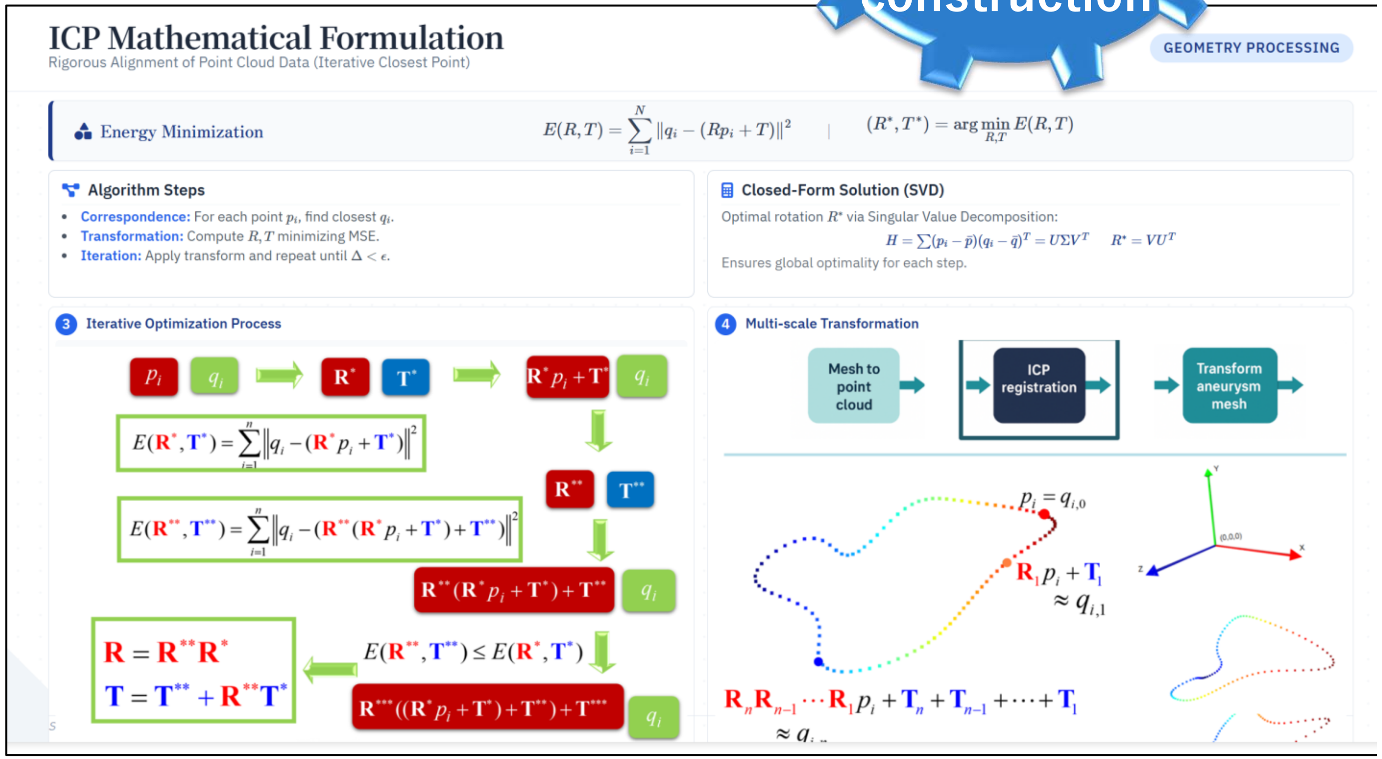

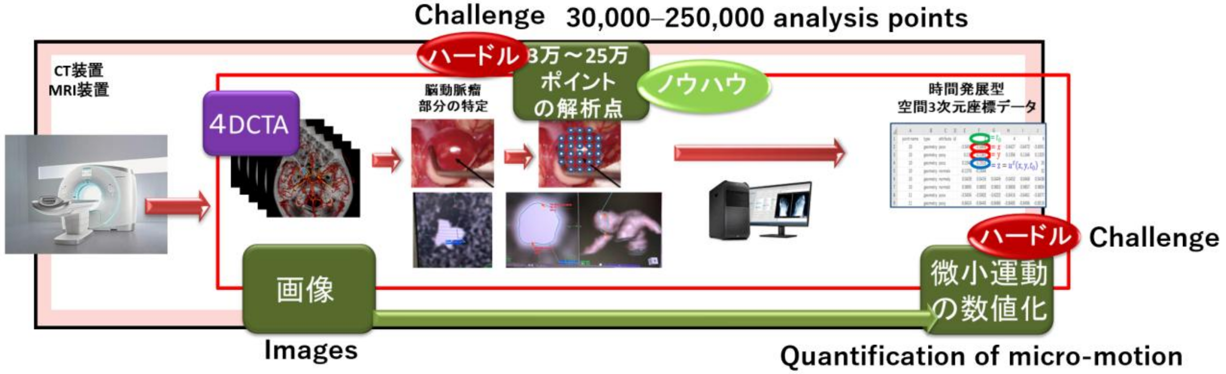

1. Problem Statement

Given source points $P=\{p_1,\ldots,p_n\}$ and target points $Q=\{q_1,\ldots,q_n\}$. Our goal is to find the optimal rigid transformation (R,t) that aligns P to Q.

2. Energy Minimization

We seek the optimal rotation matrix R and translation vector t that minimize the mean squared error (MSE):

$$E(R,t)=\sum_{i=1}^{n}\|Rp_i+t-q_i\|^2$$

3. Algorithm Steps

Step 1: Correspondence

For each point p_i, find the closest point q_k in the target set: $k=\arg\min_j\|p_i-q_j\|$

Step 2: Transformation

Compute (R,t) that minimizes the energy function using the SVD solution derived below.

Step 3: Iteration

Apply transformation $p_i\leftarrow Rp_i+t$ and repeat until convergence $\Delta E<\epsilon$.

time-evolving point cloud construction

Moving Boundary Problem - Mathematical Formulation

Mathematical Formulation (KS System)

論文

Let $d \geq 2$, $0 < T < \infty$ and $\gamma > 0$.

For $t \in (0, T]$, let $\Omega_t \subset \mathbb{R}^d$ be a bounded domain with $\partial\Omega_t \in C^2$ and set $Q_T := \bigcup_{0<t\leq T} \Omega_t \times \{t\}$.

$$
\text{(KS)} \quad \begin{cases}
\partial_t u = \Delta u - \nabla \cdot (u \nabla v) & \text{in } Q_T \\
0 = \Delta v - \gamma v + u & \text{in } Q_T \\
\partial_{n_t} u = \partial_{n_t} v = 0 & \text{on } \bigcup_{0<t<T} \partial\Omega_t \times \{t\} \\
u|_{t=0} = u_0 & \text{in } \Omega_0
\end{cases}
$$

$$M\ddot{q} + Kq + \alpha q^3 = F(t)$$

- $u = u(x,t)$: the unknown densi
- $v = v(x,t)$: the unknown concentration of chemical attractant
- $n_t = {}^{\mathsf{T}}(n_{t,1}, \ldots, n_{t,d})$: the outward normal on $\partial\Omega_t$

ALE METHOD VISUALIZATION

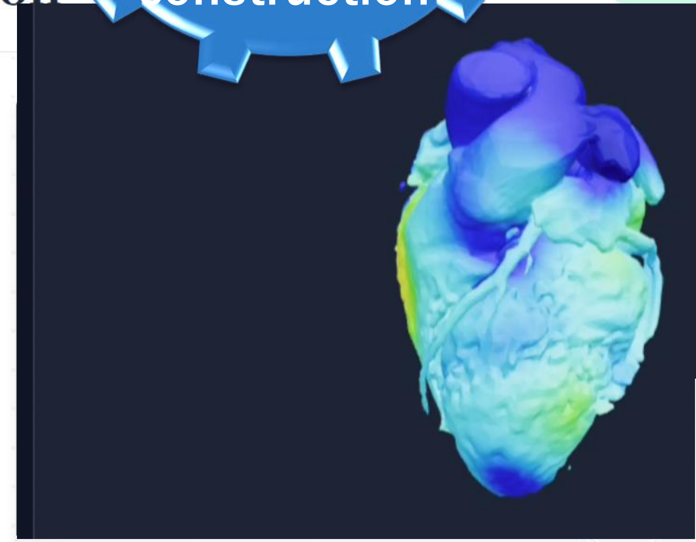

Dynamic Domain Deformation

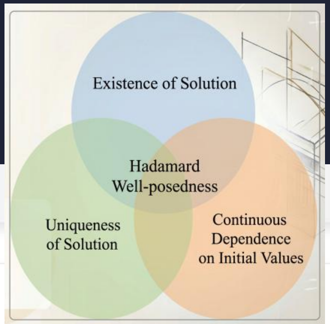

Domain Evolution Visualization

Paper1

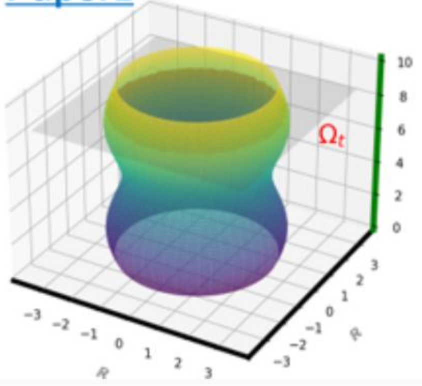

Paper2

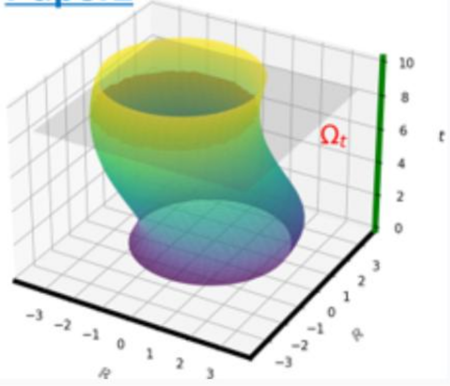

Mathematical Well-Posedness

Ensuring Simulation Stability through Rigorous Mathematical Foundations

Hadamard's Well-posedness

Defining initial/boundary conditions establishes an appropriate class of solutions, proving three critical properties for validity.

Three Fundamental Properties

- **1. Existence:** A solution exists within the function space.
- **2. Uniqueness:** The solution is unique; no physical ambiguity.
- **3. Continuous Dependence:** Small input changes yield small output changes. Corresponds to Experimental Reproducibility

→ **This mathematical guarantee is the prerequisite for numerical stability and successful clinical application.**

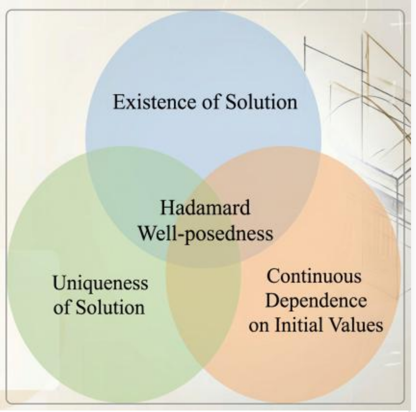

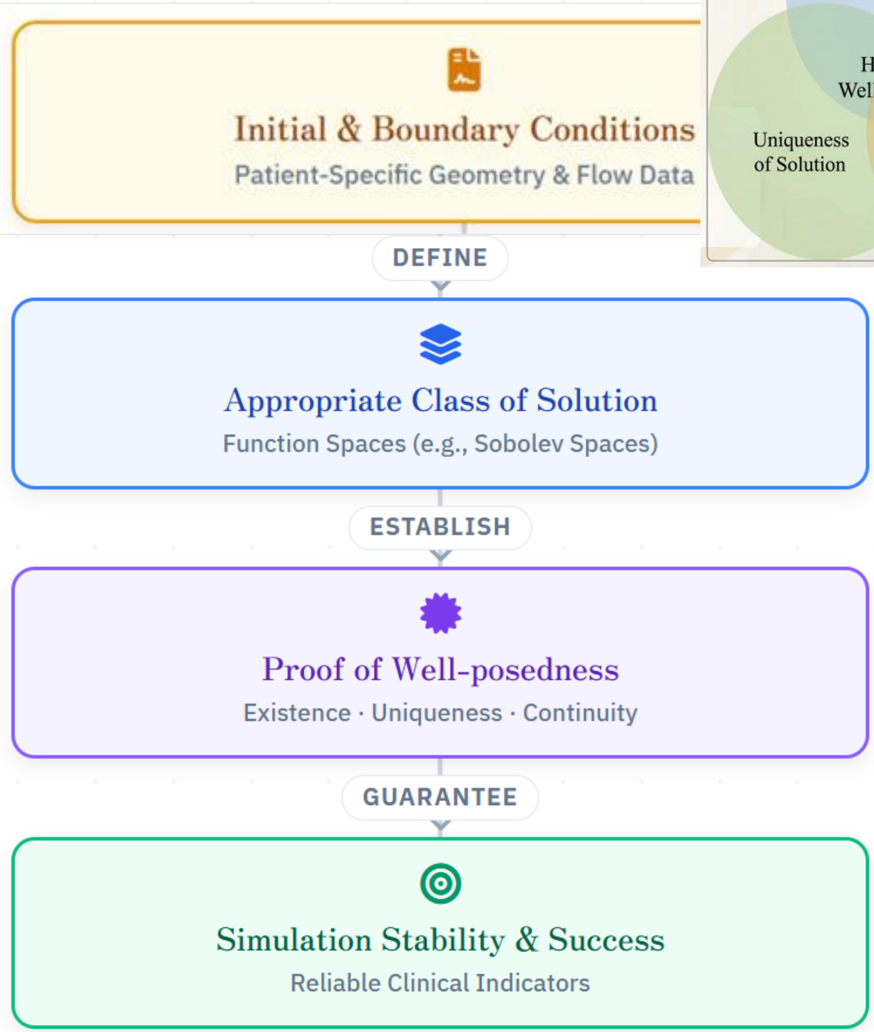

interdisciplinary research

Mathematics × Medicine × Information Science

Initial & Boundary Conditions

Patient-Specific Geometry & Flow Data

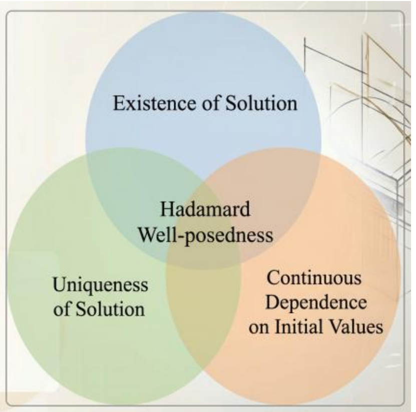

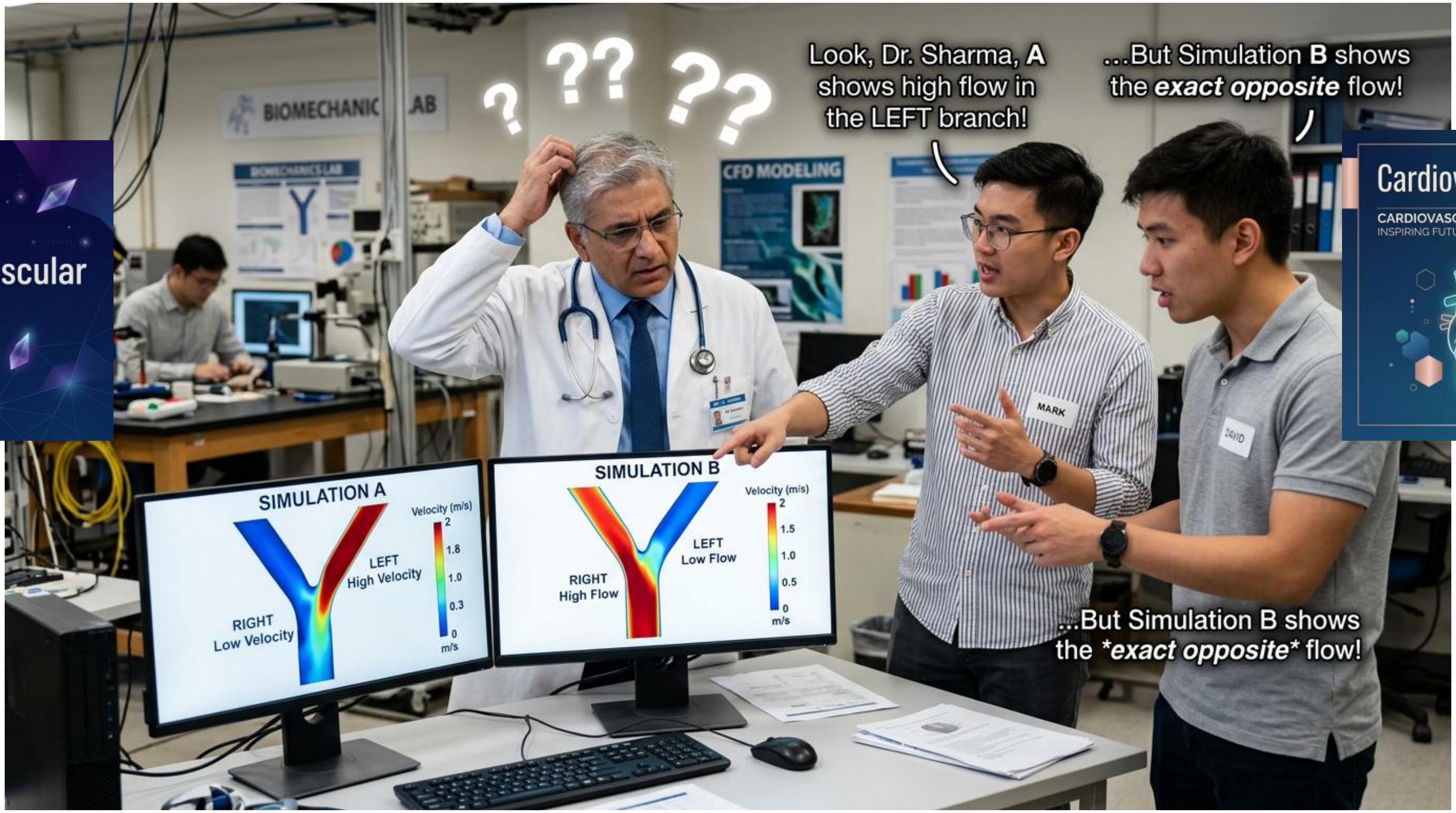

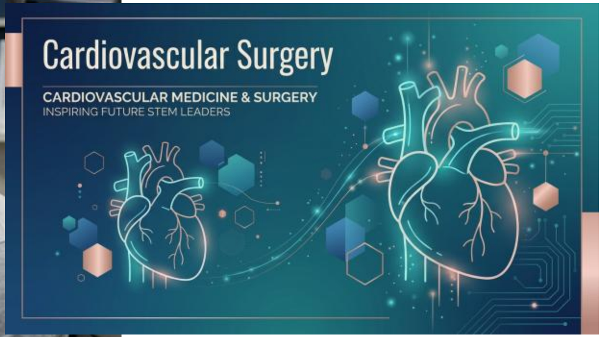

Boundary Conditions: Mathematical Significance

Defining the Interface Between Anatomy and Numerics

- ### Inflow: Dirichlet Condition

  Prescribing velocity profiles (parabolic/plug) based on clinical measurements (PC-MRI).

  $u = g(x, t)$ on Γ_{in}

- ### Wall: No-Slip / Partial Slip

  Standard hemodynamic assumption vs. complex interactions in pathological vessels.

  $u = 0$ on Γ_{wall} (Rigid wall assumption)

- ### Outflow: Resistance / Windkessel Critical

  Coupling 3D domain with 0D lumped parameter models to represent downstream vascular resistance.

  $P = R \cdot Q + C \cdot (dP/dt)$

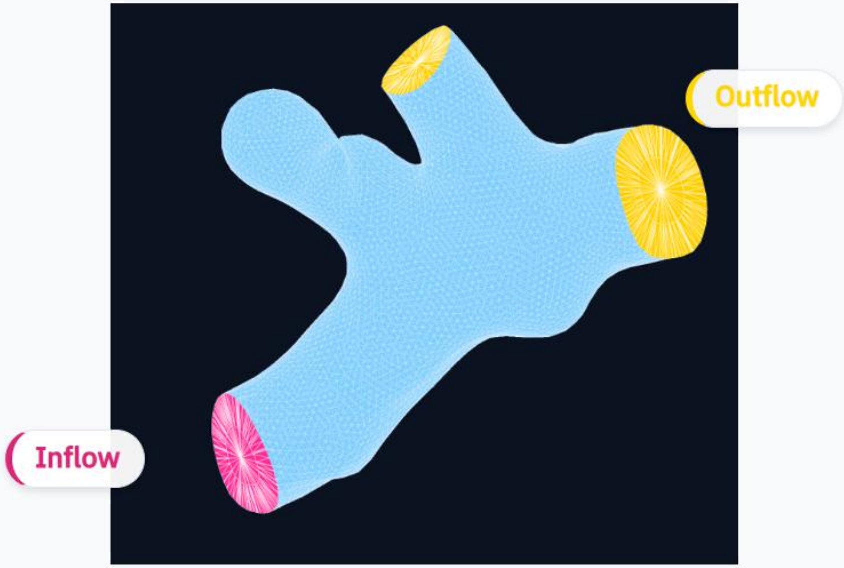

$$\frac{\partial \mathbf{u}}{\partial t} + (\mathbf{u}\cdot\nabla)\mathbf{u} = -\nabla p + \nu\Delta\mathbf{u}$$

The well-posedness of the Navier-Stokes system strictly depends on appropriate BCs on $\partial\Omega$.

Initial and Boundary Conditions

Defining the Foundation for Simulation

METHODOLOGY

1 Data Integration

Reconstruct 3D geometry from CT/MRI. Use **ICP** for multi-modal alignment and mesh smoothing.

Preprocessing

2 Initial and Boundary Conditions

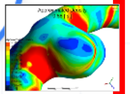

Define inflow waveforms and outflow resistance (Windkessel models) based on clinical data.

Mathematical Modeling

3 Simulation

Execute **Micropolar δ+-SPH** solver on GPU. Real-time computation of complex hemodynamics.

Core Computation

4 Indicator Evaluation

Calculate Power Loss, WSS, HFD, and pressure drops from particle data.

Post-processing

5 Multi-obj Optimization

Compare surgical options based on quantitative trade-offs (e.g., energy vs. flow balance).

Decision Support

Iterative Feedback Loop

The process is not strictly linear; **real-time visualization** allows for interactive adjustment of parameters and immediate feedback on hemodynamic impact, facilitating active dialogue with surgeons.

Micropolar Fluid Equations

Capturing Vortical Structures with Micro-rotation Degrees of Freedom

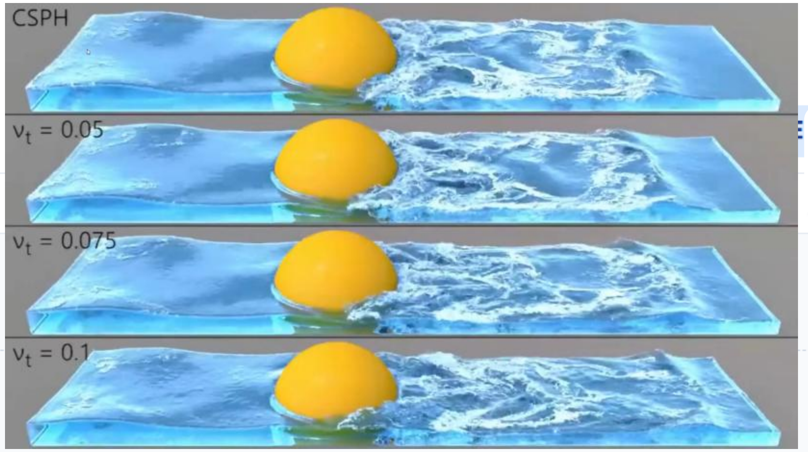

Jan Bender, Dan Koschier, Tassilo Kugelstadt and Marcel Weiler, "Turbulent Micropolar SPH Fluids with Foam", IEEE Transactions on Visualization and Computer Graphics, 2018

Coupled System for Velocity ($\mathbf{u}$) and Micro-rotation ($\mathbf{w}$)

$$\frac{\partial \mathbf{u}}{\partial t} + (\mathbf{u} \cdot \nabla)\mathbf{u} = -\frac{1}{\rho}\nabla p + \nu \Delta \mathbf{u} + \nabla \times \mathbf{w} + \mathbf{f}$$

$$\frac{\partial \mathbf{w}}{\partial t} + (\mathbf{u} \cdot \nabla)\mathbf{w} = \xi \Delta \mathbf{w} + \gamma(\nabla \times \mathbf{u} - 2\mathbf{w})$$

Physical Significance

Introduces intrinsic **micro-rotation $\mathbf{w}$** (spin) as an internal variable.

- Preserves vortical structures by reducing numerical dissipation.
- Bidirectional coupling: vorticity generates spin, spin feeds back to velocity.
- Crucial for turbulent flow features at high Reynolds numbers.

Key Parameters

γ **Transfer Coefficient (Vortex Viscosity):**
Controls the strength of coupling between macro-rotation ($\nabla \times \mathbf{u}$) and micro-rotation ($\mathbf{w}$).

ξ **Micro-inertia / Spin Viscosity:**
Governs the diffusion of micro-rotation field.

Source: Chen, Shao, Sugiyama, "GPU-accelerated micropolar δ^+-SPH framework...", Computer Physics Communications (2026)

Micropolar Fluid Model - Unified Formulation

ADVANCED FLUID DYNAMICS

Governing System

$$\frac{\partial \mathbf{u}}{\partial t} + (\mathbf{u} \cdot \nabla)\mathbf{u} = -\frac{1}{\rho}\nabla p + \nu \Delta \mathbf{u} + (\nu + \nu_r)(\nabla \times \mathbf{w}) + \mathbf{g}$$

→ Velocity Field Evolution

$$\frac{\partial \mathbf{w}}{\partial t} + (\mathbf{u} \cdot \nabla)\mathbf{w} = \gamma \Delta \mathbf{w} + \xi(\nabla \times \mathbf{u} - 2\mathbf{w}) + \mathbf{f}$$

Micro-rotation Field Evolution

in Q_T

in Q_T

on $\bigcup_{0<t<T} \partial\Omega_t \times \{t\}$

in Ω_0

DOMAIN DEFINITION

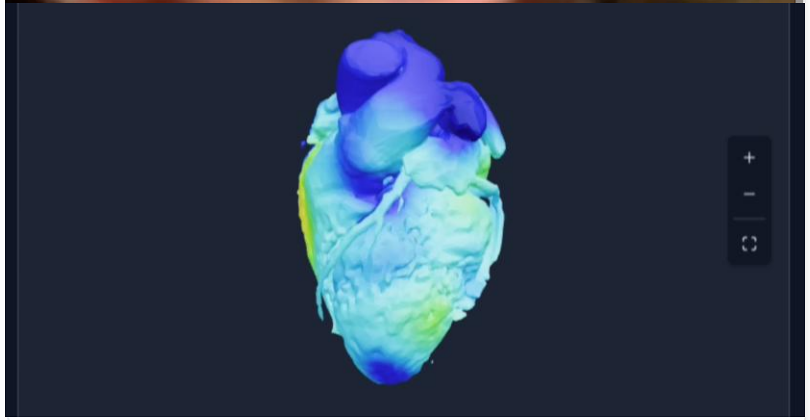

Theoretical Framework & Application

The micropolar fluid model is a theoretical framework that enables the description of complex fluid behaviors that cannot be represented by conventional Navier-Stokes equations, by introducing the degree of freedom for particle self-rotation (spin) as an internal variable. In this model, in addition to the time evolution of the velocity field **u**, an evolution equation for the micro-rotation field **w** is introduced, forming the following coupled system. In the SPH simulation example by Jan Bender et al., the variation in viscous damping behavior of surface waves is visualized by increasing ν_r (IEEE Trans. Vis. Comput. Graph., 2018).

Initial and Boundary Conditions 血流動態

Defining the Foundation for Simulation

HEMODYNAMICS

METHODOLOGY

1 Data Integration

Reconstruct 3D geometry from CT/MRI. Use **ICP** for multi-modal alignment and mesh smoothing.

Preprocessing

2 Initial and Boundary Conditions

Define inflow waveforms and outflow resistance (Windkessel models) based on clinical data.

Mathematical Modeling

3 Simulation

Execute **Micropolar δ+-SPH** solver on GPU. Real-time computation of complex hemodynamics.

Core Computation

4 Indicator Evaluation

Calculate Power Loss, WSS, HFD, and pressure drops from particle data.

Post-processing

5 Multi-obj Optimization

Compare surgical options based on quantitative trade-offs (e.g., energy vs. flow balance).

Decision Support

CFD ANALYSIS

Iterative Feedback Loop

The process is not strictly linear; **real-time visualization** allows for interactive adjustment of parameters and immediate feedback on hemodynamic impact, facilitating active dialogue with surgeons.

Numerical Methods Comparison

Selecting the Right Tool: FVM vs. FEM vs. SPH

HEMODYNAMICS

FINITE VOLUME METHOD (FVM)

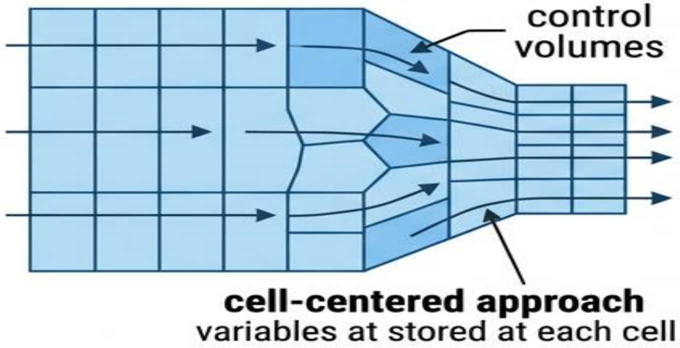

- ✔ Robust Conservation
- ✔ High Efficiency
- ✘ Complex Mesh Generation

FINITE ELEMENT METHOD (FEM)

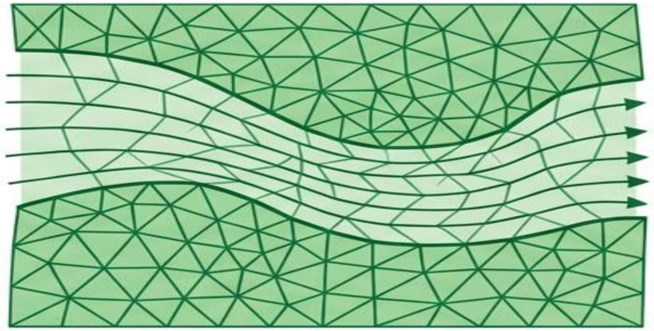

- ✔ Complex Boundaries
- ✔ Strong Mathematical Foundation
- ✘ High Computational Cost
- ✘ Conservation Issues

SMOOTHED PARTICLE HYDRODYNAMICS (SPH)

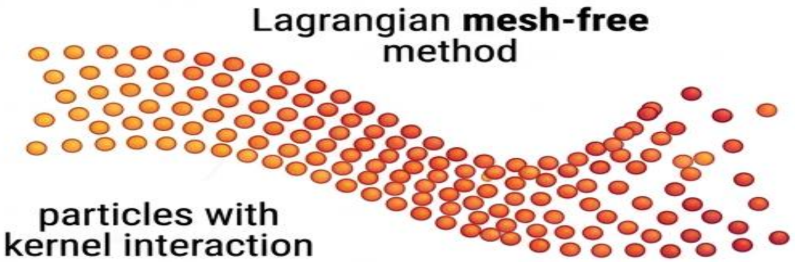

- ✔ No Mesh Needed
- ✔ Natural Free Surface Handling
- ✔ Exact Mass Conservation
- ✘ Computational Intensity
- ✘ Boundary Condition Implementation

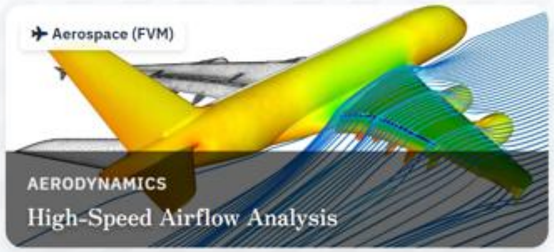

AERODYNAMICS
High-Speed Airflow Analysis

STRUCTURAL INTEGRITY
Stress & Load Simulation

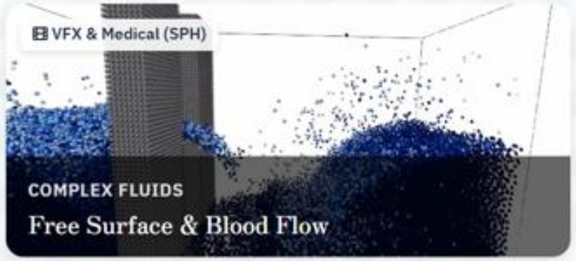

COMPLEX FLUIDS
Free Surface & Blood Flow

SPH Fundamentals - Particle-based Fluid Simulation

COMPUTATIONAL FLUID DYNAMICS

1. Kernel Approximation & Discretization

Continuous fields are approximated by interpolation using a smoothing kernel W with smoothing length h.

$$A(\mathbf{r}) \approx \sum_j \frac{m_j}{\rho_j} A_j W(\mathbf{r} - \mathbf{r}_j, h)$$

Fundamental SPH Interpolation Formula

Source: ATA Engineering, "Introducing the SPH Multiphase Model in Simcenter STAR-CCM+," https://www.ata-e.com/software/training-support/free-resources/introducing-the-sph-multiphase-model-in-simcenter-star-ccm/ (Accessed: February 2026)

2. Navier-Stokes Equations (Lagrangian Form)

$$\textbf{Continuity:}\ \frac{d\rho_i}{dt} = \sum_j m_j(\mathbf{v}_i - \mathbf{v}_j) \cdot \nabla_i W_{ij}$$

$$\textbf{Momentum:}\ \frac{d\mathbf{v}_i}{dt} = -\sum_j m_j \left(\frac{p_i}{\rho_i^2} + \frac{p_j}{\rho_j^2} + \Pi_{ij} \right) \nabla_i W_{ij} + \mathbf{g}$$

Key Characteristics & Advantages

Lagrangian Description

Mesh-free method ideal for tracking free surfaces, large deformations, and complex topology changes (e.g., splashing).

Conservation Properties

Inherently conserves mass, linear momentum, and angular momentum due to symmetric particle interactions.

Adaptive Resolution

Particles naturally concentrate in regions of interest, providing automatic adaptivity for fluid flow.

Computer Physics Communications (CPC)

Bridging Mathematics, Physics, and Advanced Software

JOURNAL INTRODUCTION

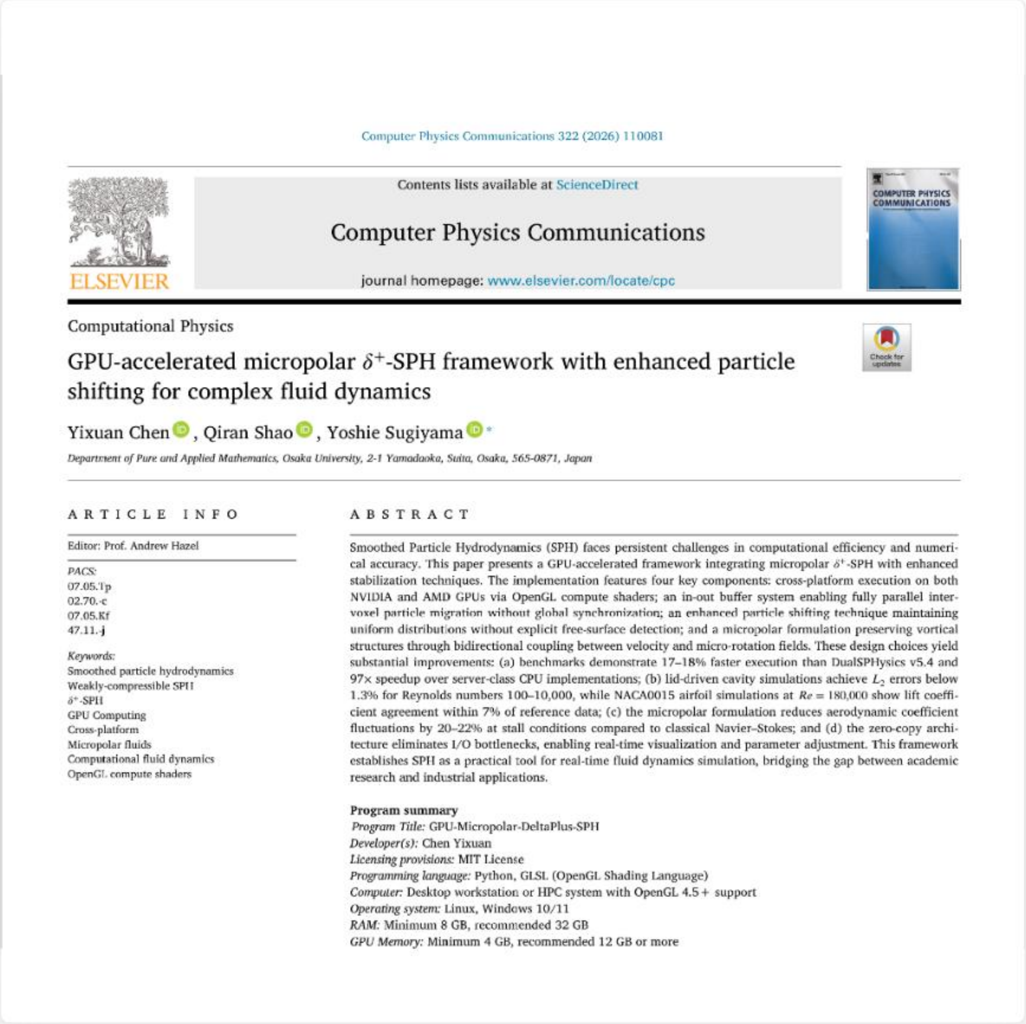

Computer Physics Communications 322 (2026) 110081

Contents lists available at ScienceDirect

Computer Physics Communications

journal homepage: www.elsevier.com/locate/cpc

ELSEVIER

Computational Physics

GPU-accelerated micropolar δ^+-SPH framework with enhanced particle shifting for complex fluid dynamics

Yixuan Chen, Qiran Shao, Yoshie Sugiyama *

Department of Pure and Applied Mathematics, Osaka University, 2-1 Yamadaoka, Suita, Osaka, 565-0871, Japan

A R T I C L E I N F O

Editor: Prof. Andrew Hazel

PACS:
07.05.Tp
02.70.-c
07.05.Kf
47.11.-j

Keywords:
Smoothed particle hydrodynamics
Weakly-compressible SPH
δ^+-SPH
GPU Computing
Cross-platform
Micropolar fluids
Computational fluid dynamics
OpenGL compute shaders

A B S T R A C T

Smoothed Particle Hydrodynamics (SPH) faces persistent challenges in computational efficiency and numerical accuracy. This paper presents a GPU-accelerated framework integrating micropolar δ^+-SPH with enhanced stabilization techniques. The implementation features four key components: cross-platform execution on both NVIDIA and AMD GPUs via OpenGL compute shaders; an in-out buffer system enabling fully parallel inter-voxel particle migration without global synchronization; an enhanced particle shifting technique maintaining uniform distributions without explicit free-surface detection; and a micropolar formulation preserving vortical structures through bidirectional coupling between velocity and micro-rotation fields. These design choices yield substantial improvements: (a) benchmarks demonstrate 17–18% faster execution than DualSPHysics v5.4 and 97× speedup over server-class CPU implementations; (b) lid-driven cavity simulations achieve L_2 errors below 1.3% for Reynolds numbers 100–10,000, while NACA0015 airfoil simulations at $Re = 180{,}000$ show lift coefficient agreement within 7% of reference data; (c) the micropolar formulation reduces aerodynamic coefficient fluctuations by 20–22% at stall conditions compared to classical Navier–Stokes; and (d) the zero-copy architecture eliminates I/O bottlenecks, enabling real-time visualization and parameter adjustment. This framework establishes SPH as a practical tool for real-time fluid dynamics simulation, bridging the gap between academic research and industrial applications.

Program summary
Program Title: GPU-Micropolar-DeltaPlus-SPH
Developer(s): Chen Yixuan
Licensing provisions: MIT License
Programming language: Python, GLSL (OpenGL Shading Language)
Computer: Desktop workstation or HPC system with OpenGL 4.5+ support
Operating system: Linux, Windows 10/11
RAM: Minimum 8 GB, recommended 32 GB
GPU Memory: Minimum 4 GB, recommended 12 GB or more

The Premier Journal for Computational Physics

ELSEVIER

- **High Impact & Authority:** A top-tier venue for algorithmic breakthroughs. The global standard for publishing Advanced Computational Methods.
- **Code is Mandatory:** Uniquely requires the publication of source code (GitHub/GitLab integration), ensuring **Full Reproducibility** of results.
- **Open Access:** Research is accessible worldwide, maximizing visibility for advanced frameworks like GPU-SPH.

KEY OPPORTUNITY

A Pathway for Mathematicians & Students

- **Bridging Theory & Practice:** Mathematics researchers can publish impactful papers by providing robust numerical implementations of rigorous theories (e.g., Micropolar fluids).
- **Empowering Students:** A proven track record for student-led research. Developing reliable software for mathematical models is a highly valued contribution, opening doors to top-tier publications.

interdisciplinary research

Mathematics × Medicine × Information Science

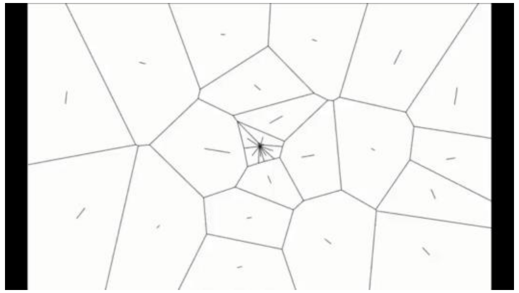

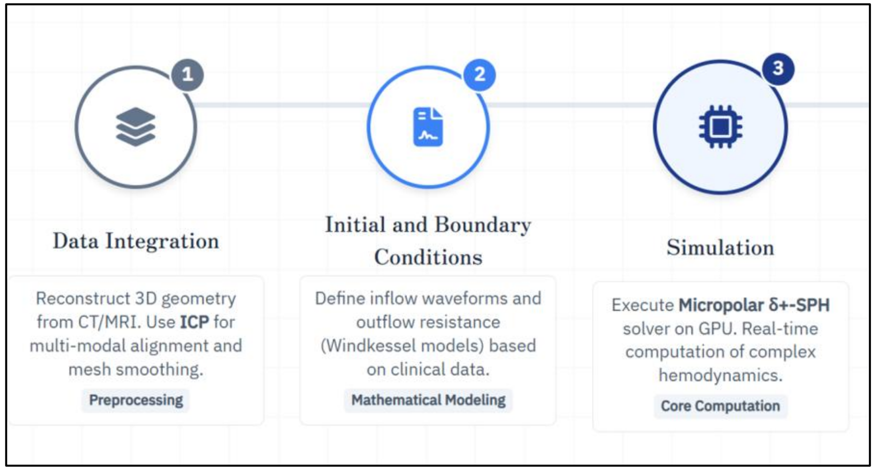

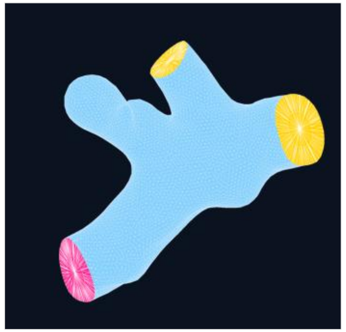

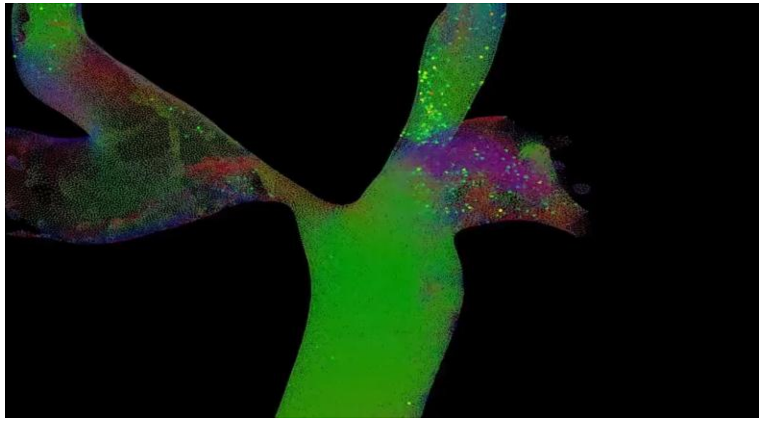

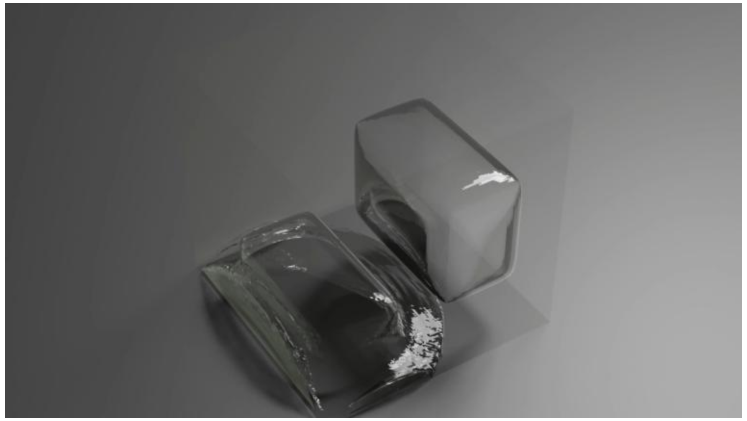

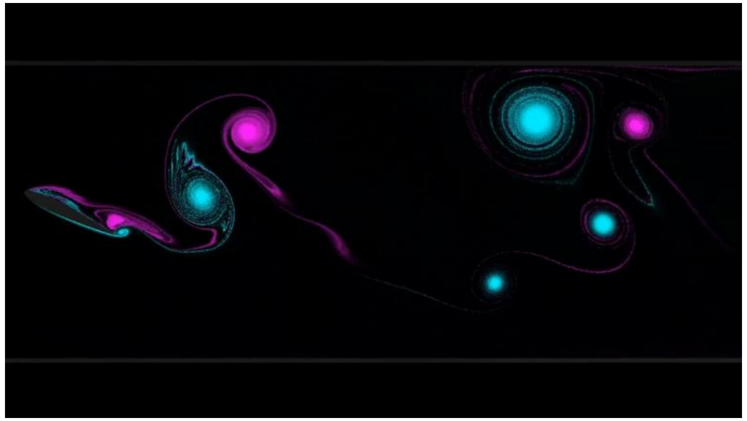

Initial and Boundary Conditions

Defining the Foundation for Simulation

METHODOLOGY

1

Data Integration

Reconstruct 3D geometry from CT/MRI. Use **ICP** for multi-modal alignment and mesh smoothing.

Preprocessing

2

Initial and Boundary Conditions

Define inflow waveforms and outflow resistance (Windkessel models) based on clinical data.

Mathematical Modeling

3

Simulation

Execute **Micropolar δ+-SPH** solver on GPU. Real-time computation of complex hemodynamics.

Core Computation

4

Indicator Evaluation

Calculate Power Loss, WSS, HFD, and pressure drops from particle data.

Post-processing

5

Multi-obj Optimization

Compare surgical options based on quantitative trade-offs (e.g., energy vs. flow balance).

Decision Support

Iterative Feedback Loop

The process is not strictly linear; **real-time visualization** allows for interactive adjustment of parameters and immediate feedback on hemodynamic impact, facilitating active dialogue with surgeons.

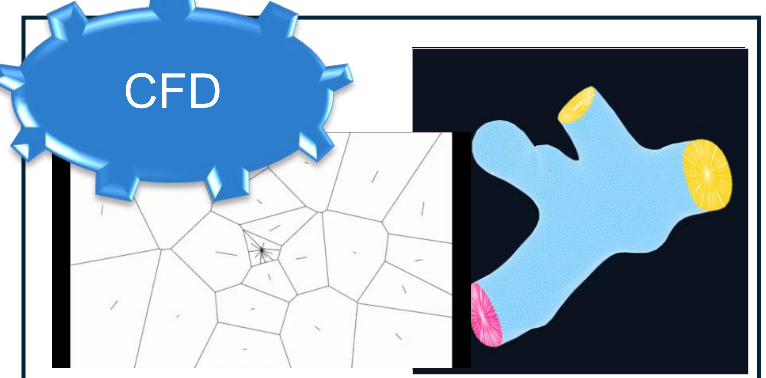

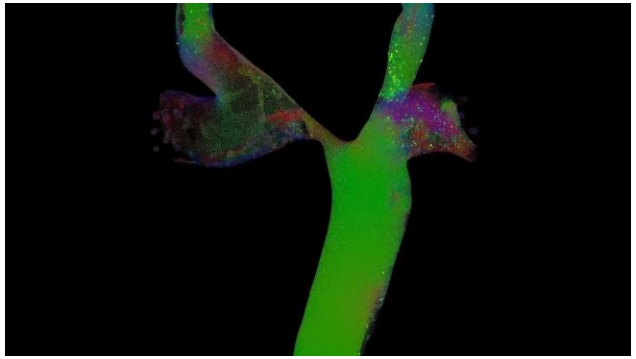

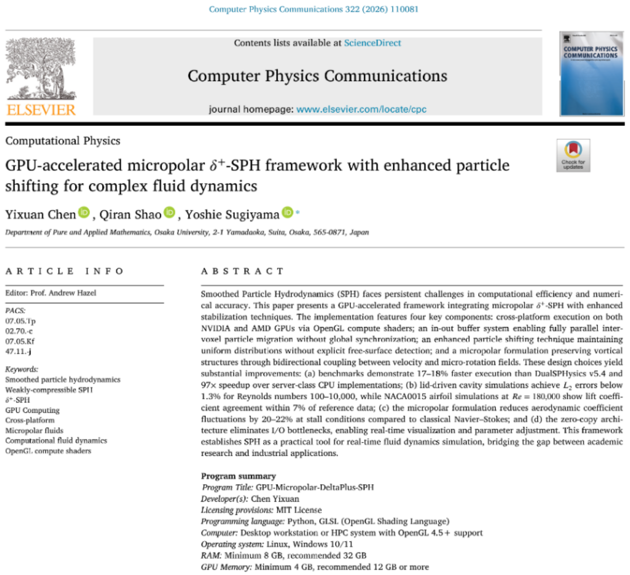
Computer Physics Communications 322 (2026) 110081

Contents lists available at ScienceDirect

Computer Physics Communications

journal homepage: www.elsevier.com/locate/cpc

Computational Physics

GPU-accelerated micropolar δ^+-SPH framework with enhanced particle shifting for complex fluid dynamics

Yixuan Chen, Qiran Shao, Yoshie Sugiyama *

Department of Pure and Applied Mathematics, Osaka University, 2-1 Yamadaoka, Suita, Osaka, 565-0871, Japan

ARTICLE INFO

Editor: Prof. Andrew Hazel

PACS:
07.05.Tp
02.70.-c
07.05.Kf
47.11.-j

Keywords:
Smoothed particle hydrodynamics
Weakly-compressible SPH
δ^+-SPH
GPU Computing
Cross-platform
Micropolar fluids
Computational fluid dynamics
OpenGL compute shaders

ABSTRACT

Smoothed Particle Hydrodynamics (SPH) faces persistent challenges in computational efficiency and numerical accuracy. This paper presents a GPU-accelerated framework integrating micropolar δ^+-SPH with enhanced stabilization techniques. The implementation features four key components: cross-platform execution on both NVIDIA and AMD GPUs via OpenGL compute shaders; an in-out buffer system enabling fully parallel inter-voxel particle migration without global synchronization; an enhanced particle shifting technique maintaining uniform distributions without explicit free-surface detection; and a micropolar formulation preserving vortical structures through bidirectional coupling between velocity and micro-rotation fields. These design choices yield substantial improvements: (a) benchmarks demonstrate 17–18% faster execution than DualSPHysics v5.4 and 97× speedup over server-class CPU implementations; (b) lid-driven cavity simulations achieve L_2 errors below 1.3% for Reynolds numbers 100–10,000, while NACA0015 airfoil simulations at $Re = 180{,}000$ show lift coefficient agreement within 7% of reference data; (c) the micropolar formulation reduces aerodynamic coefficient fluctuations by 20–22% at stall conditions compared to classical Navier–Stokes; and (d) the zero-copy architecture eliminates I/O bottlenecks, enabling real-time visualization and parameter adjustment. This framework establishes SPH as a practical tool for real-time fluid dynamics simulation, bridging the gap between academic research and industrial applications.

Program summary
Program Title: GPU-Micropolar-DeltaPlus-SPH
Developer(s): Chen Yixuan
Licensing provisions: MIT License
Programming language: Python, GLSL (OpenGL Shading Language)
Computer: Desktop workstation or HPC system with OpenGL 4.5+ support
Operating system: Linux, Windows 10/11
RAM: Minimum 8 GB, recommended 32 GB
GPU Memory: Minimum 4 GB, recommended 12 GB or more

CREST

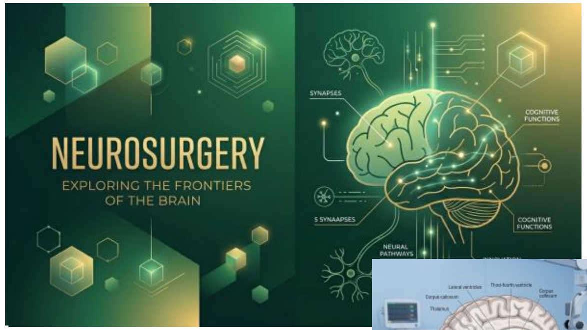

Patent Patent Patent Patent Patent

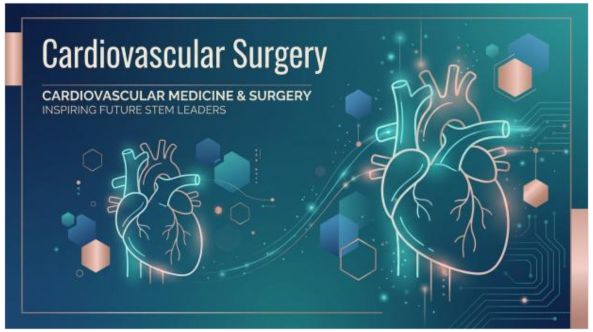

Patent Patent

Patent

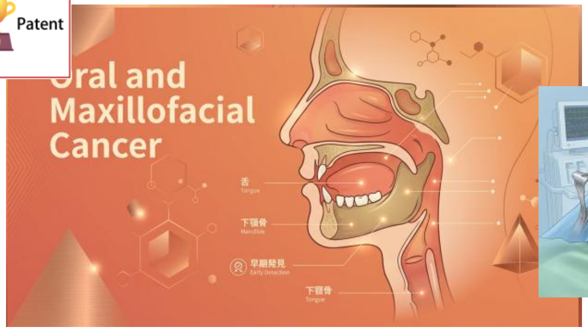

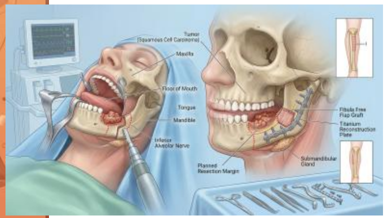

interdisciplinary research

Mathematics × Medicine × Information Science

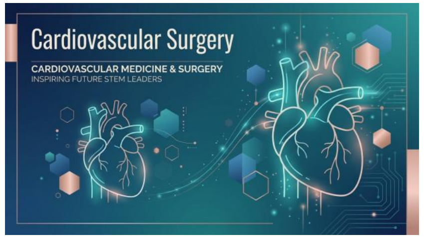

特許 特許

CFD Analysis: Visualizing Invisible Flow

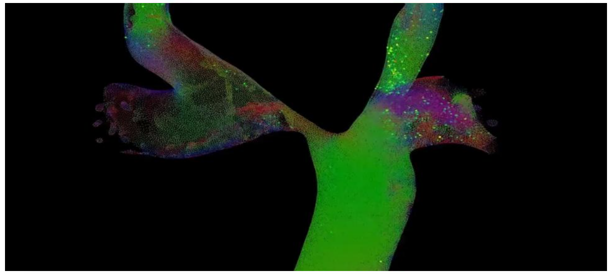

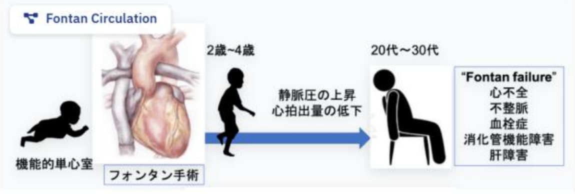

Surgical Planning

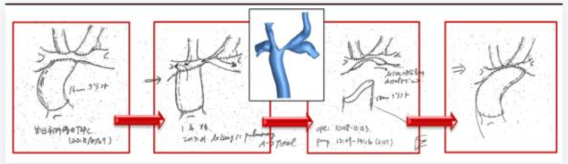

Key Indicators

LPA/RPA Flow Distribution
Evaluating the balance of blood flow to the left and right pulmonary arteries to prevent pulmonary arteriovenous malformations.

Power Loss Analysis
Quantifying energy efficiency to minimize cardiac workload and optimize hemodynamic performance.

Surgical Planning Support
Pre-operative simulation allows for the virtual testing of graft geometries to determine the optimal surgical strategy.

Congenital Heart Disease | Research Objective | Proposal of surgical strategy aimed at optimizing pulmonary blood flow in congenital heart disease based on objective indicators

Monthly Regular Meeting

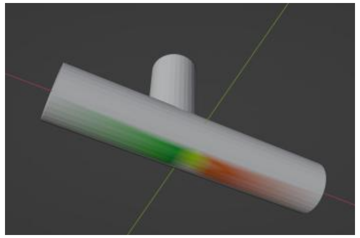

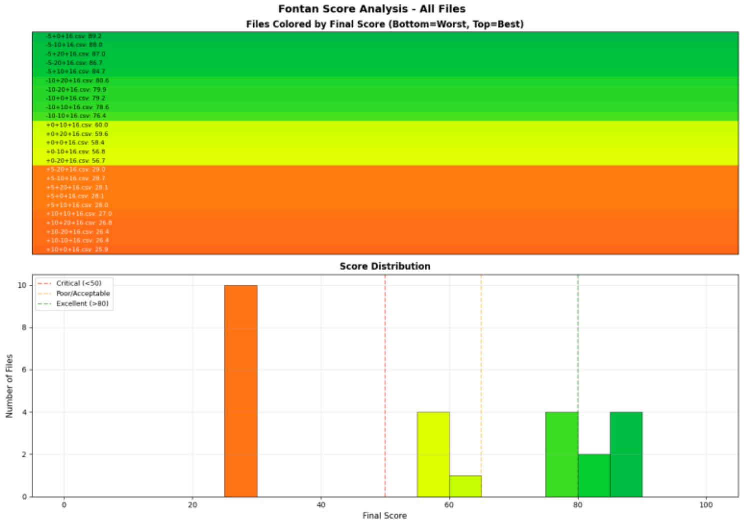

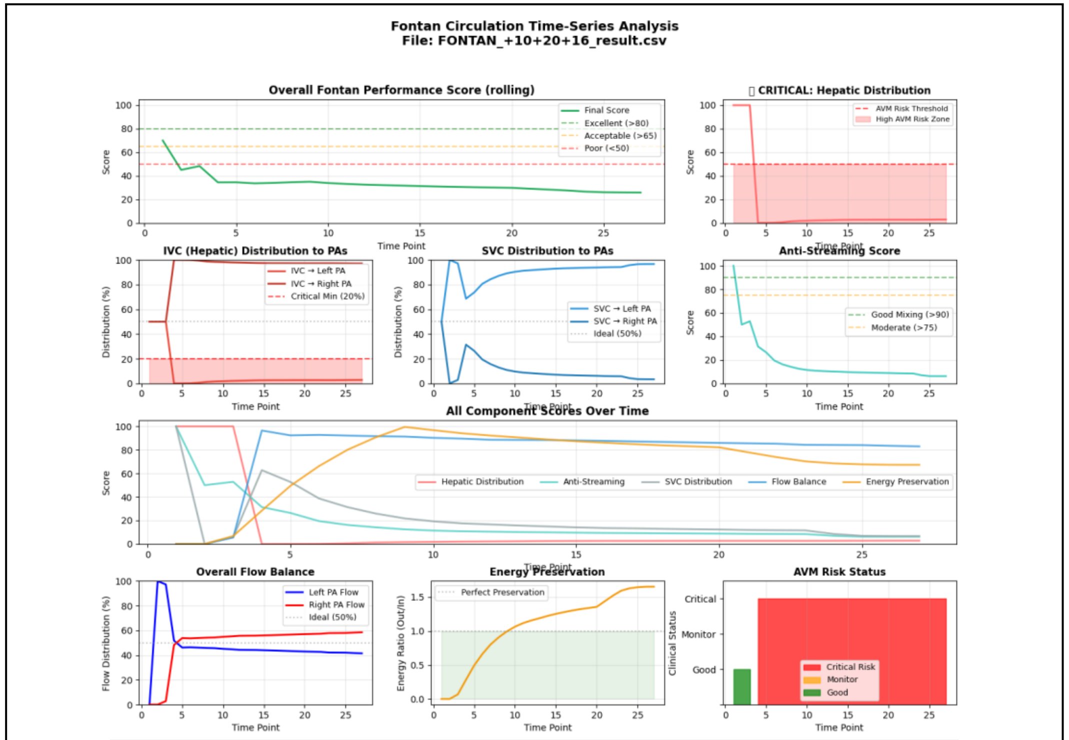

先天性心疾患 | 研究目的 | 客観的指標に基づく先天性心疾患の肺血流最適化を目指した手術戦略の立案

CFD

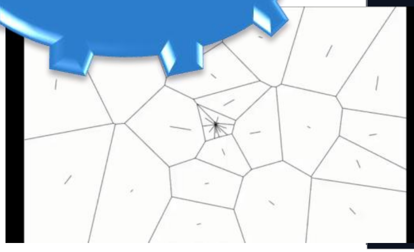

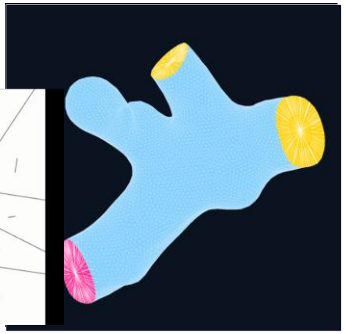

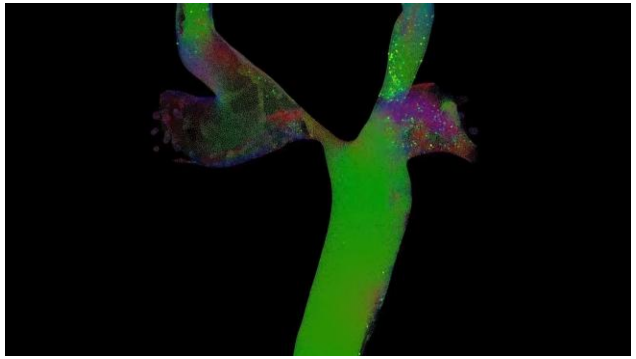

Computer Physics Communications 322 (2026) 110081

Contents lists available at ScienceDirect

Computer Physics Communications

journal homepage: www.elsevier.com/locate/cpc

ELSEVIER

Computational Physics

GPU-accelerated micropolar δ^{+}-SPH framework with enhanced particle shifting for complex fluid dynamics

Yixuan Chen, Qiran Shao, Yoshie Sugiyama *

Department of Pure and Applied Mathematics, Osaka University, 2-1 Yamadaoka, Suita, Osaka, 565-0871, Japan

A R T I C L E   I N F O

Editor: Prof. Andrew Hazel

PACS:
07.05.Tp
02.70.-c
07.05.Kf
47.11.-j

Keywords:
Smoothed particle hydrodynamics
Weakly-compressible SPH
δ^{+}-SPH
GPU Computing
Cross-platform
Micropolar fluids
Computational fluid dynamics
OpenGL compute shaders

A B S T R A C T

Smoothed Particle Hydrodynamics (SPH) faces persistent challenges in computational efficiency and numerical accuracy. This paper presents a GPU-accelerated framework integrating micropolar δ^{+}-SPH with enhanced stabilization techniques. The implementation features four key components: cross-platform execution on both NVIDIA and AMD GPUs via OpenGL compute shaders; an in-out buffer system enabling fully parallel inter-voxel particle migration without global synchronization; an enhanced particle shifting technique maintaining uniform distributions without explicit free-surface detection; and a micropolar formulation preserving vortical structures through bidirectional coupling between velocity and micro-rotation fields. These design choices yield substantial improvements: (a) benchmarks demonstrate 17–18% faster execution than DualSPHysics v5.4 and 97× speedup over server-class CPU implementations; (b) lid-driven cavity simulations achieve L_2 errors below 1.3% for Reynolds numbers 100–10,000, while NACA0015 airfoil simulations at $Re = 180{,}000$ show lift coefficient agreement within 7% of reference data; (c) the micropolar formulation reduces aerodynamic coefficient fluctuations by 20–22% at stall conditions compared to classical Navier–Stokes; and (d) the zero-copy architecture eliminates I/O bottlenecks, enabling real-time visualization and parameter adjustment. This framework establishes SPH as a practical tool for real-time fluid dynamics simulation, bridging the gap between academic research and industrial applications.

Program summary
Program Title: GPU-Micropolar-DeltaPlus-SPH
Developer(s): Chen Yixuan
Licensing provisions: MIT License
Programming language: Python, GLSL (OpenGL Shading Language)
Computer: Desktop workstation or HPC system with OpenGL 4.5 + support
Operating system: Linux, Windows 10/11
RAM: Minimum 8 GB, recommended 32 GB
GPU Memory: Minimum 4 GB, recommended 12 GB or more

CREST

1 2 3

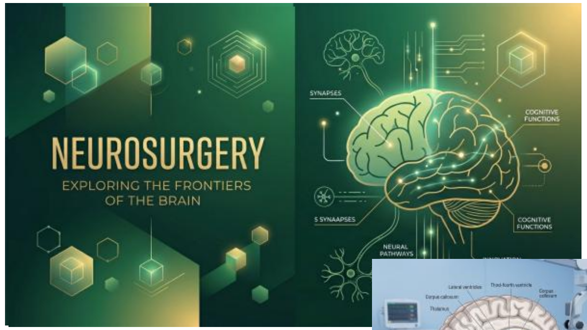

Patent Patent Patent Patent Patent

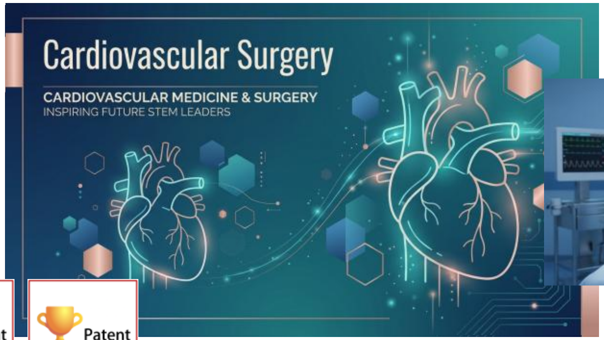

Patent Patent

Patent

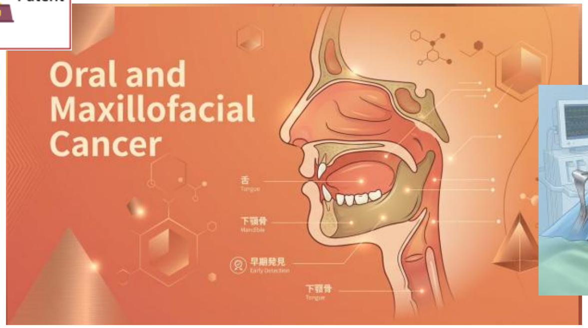

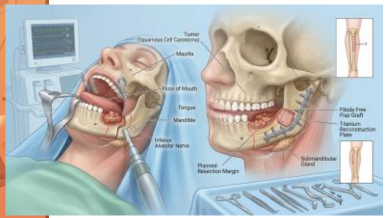

interdisciplinary research

Mathematics × Medicine × Information Science

Patent Patent Patent Patent Patent

CFD-Based Cerebral Aneurysm Vulnerability Prediction ❶

DERIVATION: FROM FUNDAMENTAL PHYSICS TO CLINICAL INDICATOR

1. Momentum Conservation

$$\rho\left(\frac{\partial \mathbf{u}}{\partial t} + (\mathbf{u}\cdot\nabla)\mathbf{u} - \mathbf{g}\right) = -\nabla P + \mu\nabla^2\mathbf{u}$$

→ Transform

2. Force Imbalance → Effective Density

$$\rho \approx \frac{|-\nabla P + \mu\nabla^2\mathbf{u}|}{|\frac{\partial \mathbf{u}}{\partial t} + (\mathbf{u}\cdot\nabla)\mathbf{u} - \mathbf{g}|}$$

→ Time Avg

3. Final Indicator: Approximated Density

$$\mathrm{AAD} = \frac{1}{T}\int_0^T \frac{|\mathbf{F}_{pressure} + \mathbf{F}_{viscous}|}{|\mathbf{a}_{inertial}|}\,dt$$

$\mathbf{F}_{pressure}$: Pressure term $(-\nabla P)$

$\mathbf{F}_{viscous}$: Viscous term $(\mu\nabla^2\mathbf{u})$

$\mathbf{a}_{inertial}$: Inertial term $(\frac{\partial \mathbf{u}}{\partial t} + (\mathbf{u}\cdot\nabla)\mathbf{u} - \mathbf{g})$

TRADITIONAL CFD INDICATORS

WSS (Wall Shear Stress)	OSI (Oscillatory Shear)
TAWSS (Time-Avg WSS)	RRT (Residence Time)
WSSG (Gradient)	SCI (Shear Conc.)

»

PHYSICALLY EXPLAINABLE ADVANTAGE

- **Explainable Physics:** Derived directly from NS equations, representing local force/inertia balance.
- **Sensitivity:** Detects "virtual density" drops indicating stagnation zones prone to degradation.
- **Clinical Correlation:** Matches intraoperative thinning points better than WSS.

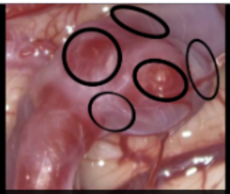

Intraoperative Validation (Red Thinning Areas) CLINICAL REALITY

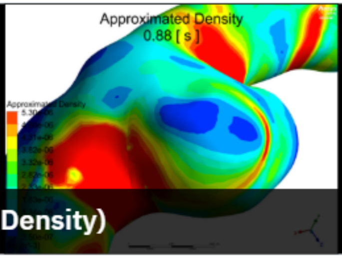

CFD Prediction (Approximated Density) SIMULATION

interdisciplinary research

Mathematics × Medicine × Information Science

Patent Patent Patent Patent Patent

AI-Based Vulnerability Prediction ❷

Aneurysm Visualization

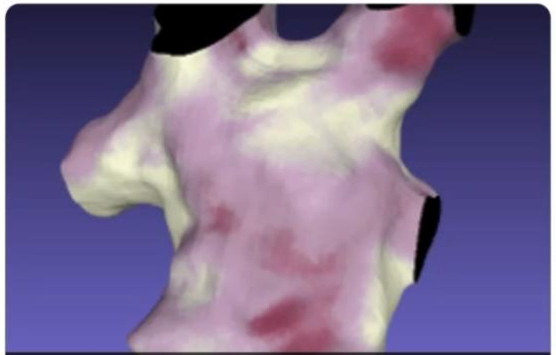

Point Cloud Geometry

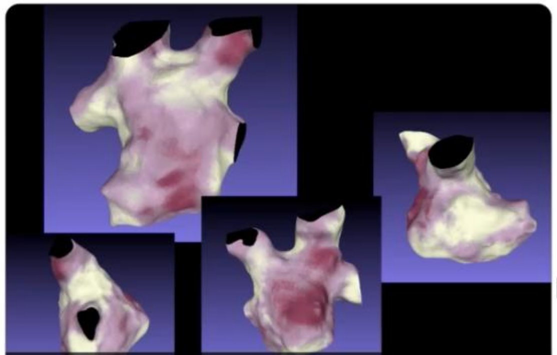

Feature Extraction

■Pattern1 変位-加速度
R—X G—Y B—Z

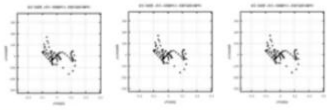

■Pattern 2 変位-速度
R—X G—Y B—Z

■Pattern 3 加速度-速度
R—X G—Y B—Z

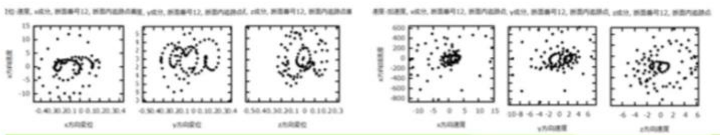

Physics-Based AI Method

1. Force
$\mathbf{F}_{ext}$

↓

2. Physics Law
$\mathbf{F} = m\mathbf{a}$

↓

3. Mass Est.
$m \approx |\mathbf{F}|/|\mathbf{a}|$

Duffing Equation

$$M\ddot{q} + C\dot{q} + Kq + \alpha q^3 = \gamma\cos(\omega t)$$

ダフィング(Duffing)振動子の動き

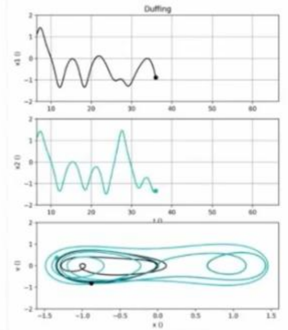

JST CREST RESEARCH TIMELINE

2019 — 2020 Point Cloud — 2022 — 2026 Clinical

Binary Classification: Ruptured vs Unruptured Aneurysms

AI CLASSIFICATION MODEL

AI Tool Development Workflow

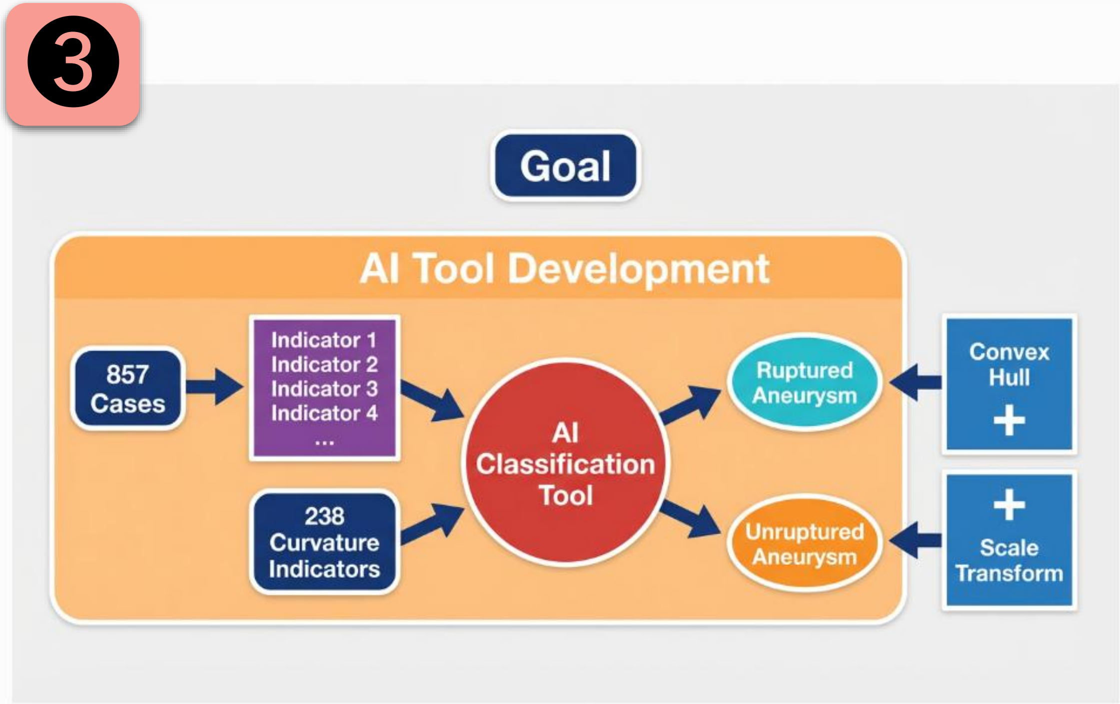

Development pipeline analyzing **857 clinical cases**. We extracted **238 geometric curvature indicators**, utilizing Convex Hull and scale transformations to train a robust classification tool.

Comprehensive Model Evaluation

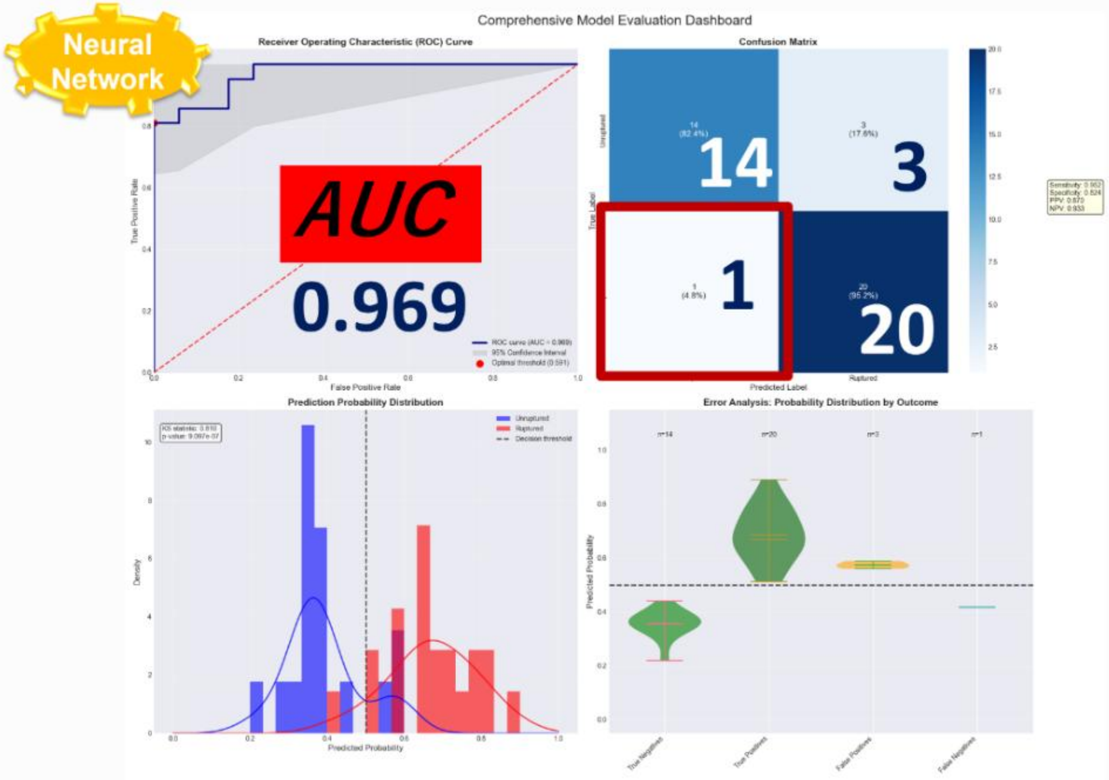

The model demonstrates high diagnostic performance with an **AUC of 0.969**. The confusion matrix and probability distributions confirm strong separation between ruptured (red) and unruptured (blue) classes.

Geometric Curvature Indicators for Rupture Prediction

VERIFIED PERFORMANCE

❸

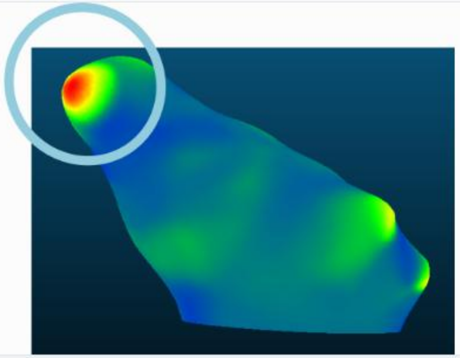

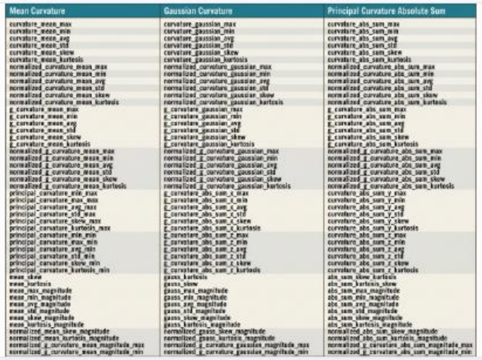

Mean Curvature	Gaussian Curvature	Principal Curvature Absolute Sum
curvature_mean_max	curvature_gaussian_max	curvature_abs_sum_max
curvature_mean_min	curvature_gaussian_min	curvature_abs_sum_min
curvature_mean_avg	curvature_gaussian_avg	curvature_abs_sum_avg
curvature_mean_std	curvature_gaussian_std	curvature_abs_sum_std
curvature_mean_skew	curvature_gaussian_skew	curvature_abs_sum_skew
curvature_mean_kurtosis	curvature_gaussian_kurtosis	curvature_abs_sum_kurtosis
normalized_curvature_mean_max	normalized_curvature_gaussian_max	normalized_curvature_abs_sum_max
normalized_curvature_mean_min	normalized_curvature_gaussian_min	normalized_curvature_abs_sum_min
normalized_curvature_mean_avg	normalized_curvature_gaussian_avg	normalized_curvature_abs_sum_avg
normalized_curvature_mean_std	normalized_curvature_gaussian_std	normalized_curvature_abs_sum_std
normalized_curvature_mean_skew	normalized_curvature_gaussian_skew	normalized_curvature_abs_sum_skew
normalized_curvature_mean_kurtosis	normalized_curvature_gaussian_kurtosis	normalized_curvature_abs_sum_kurtosis
g_curvature_mean_max	g_curvature_gaussian_max	g_curvature_abs_sum_max
g_curvature_mean_min	g_curvature_gaussian_min	g_curvature_abs_sum_min
g_curvature_mean_avg	g_curvature_gaussian_avg	g_curvature_abs_sum_avg
g_curvature_mean_std	g_curvature_gaussian_std	g_curvature_abs_sum_std
g_curvature_mean_skew	g_curvature_gaussian_skew	g_curvature_abs_sum_skew
g_curvature_mean_kurtosis	g_curvature_gaussian_kurtosis	g_curvature_abs_sum_kurtosis
normalized_g_curvature_mean_max	normalized_g_curvature_gaussian_max	normalized_g_curvature_abs_sum_max
normalized_g_curvature_mean_min	normalized_g_curvature_gaussian_min	normalized_g_curvature_abs_sum_min
normalized_g_curvature_mean_avg	normalized_g_curvature_gaussian_avg	normalized_g_curvature_abs_sum_avg
normalized_g_curvature_mean_std	normalized_g_curvature_gaussian_std	normalized_g_curvature_abs_sum_std
normalized_g_curvature_mean_skew	normalized_g_curvature_gaussian_skew	normalized_g_curvature_abs_sum_skew
normalized_g_curvature_mean_kurtosis	normalized_g_curvature_gaussian_kurtosis	normalized_g_curvature_abs_sum_kurtosis
principal_curvature_min_max	g_curvature_abs_sum_x_max	curvature_abs_sum_y_max
principal_curvature_max_max	g_curvature_abs_sum_x_min	curvature_abs_sum_y_min
principal_curvature_avg_max	g_curvature_abs_sum_x_avg	curvature_abs_sum_y_avg
principal_curvature_std_max	g_curvature_abs_sum_x_std	curvature_abs_sum_y_std
principal_curvature_skew_max	g_curvature_abs_sum_x_skew	curvature_abs_sum_y_skew
principal_curvature_kurtosis_max	g_curvature_abs_sum_x_kurtosis	curvature_abs_sum_y_kurtosis
principal_curvature_min_min	g_curvature_abs_sum_z_max	curvature_abs_sum_z_max
principal_curvature_max_min	g_curvature_abs_sum_z_min	curvature_abs_sum_z_min
principal_curvature_avg_min	g_curvature_abs_sum_z_avg	curvature_abs_sum_z_avg
principal_curvature_std_min	g_curvature_abs_sum_z_std	curvature_abs_sum_z_std
principal_curvature_skew_min	g_curvature_abs_sum_z_skew	curvature_abs_sum_z_skew
principal_curvature_kurtosis_min	g_curvature_abs_sum_z_kurtosis	curvature_abs_sum_z_kurtosis
mean_skew	gauss_kurtosis	abs_sum_skew_kurtosis
mean_kurtosis	gauss_skew	abs_sum_kurtosis_skew
mean_max_magnitude	gauss_max_magnitude	abs_sum_max_magnitude
mean_min_magnitude	gauss_min_magnitude	abs_sum_min_magnitude
mean_avg_magnitude	gauss_avg_magnitude	abs_sum_avg_magnitude
mean_std_magnitude	gauss_std_magnitude	abs_sum_std_magnitude
mean_skew_magnitude	gauss_skew_magnitude	abs_sum_skew_magnitude
mean_kurtosis_magnitude	gauss_kurtosis_magnitude	abs_sum_kurtosis_magnitude
normalized_mean_skew_magnitude	normalized_gauss_skew_magnitude	normalized_abs_sum_skew_magnitude
normalized_mean_kurtosis_magnitude	normalized_gauss_kurtosis_magnitude	normalized_abs_sum_kurtosis_magnitude
normalized_g_curvature_mean_magnitude_max	normalized_g_curvature_gaussian_magnitude_max	normalized_g_curvature_abs_sum_magnitude_max
normalized_g_curvature_mean_magnitude_min	normalized_g_curvature_gaussian_magnitude_min	normalized_g_curvature_abs_sum_magnitude_min

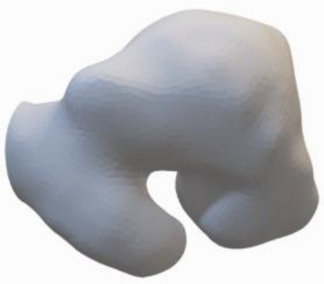

3D Reconstruction

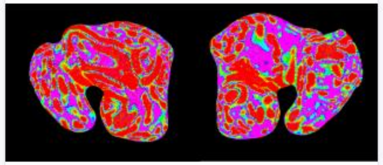

Curvature Map

Feature Importance Flow

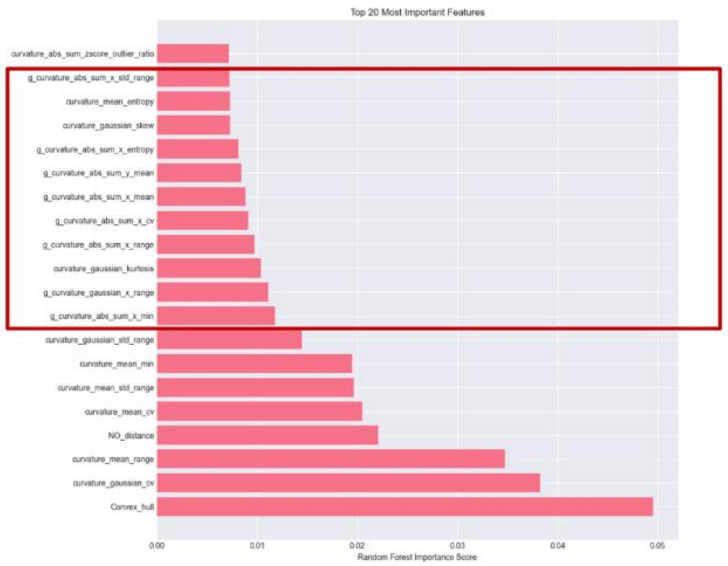

Top 20 Features

Internal Validation Results

Our internal validation study confirms the exceptional predictive power of geometric curvature indicators. By analyzing 238 morphological features, the model achieved outstanding performance in distinguishing ruptured from unruptured aneurysms.

AUC: 0.969

This result validates that **purely morphological features** contain sufficient information for highly

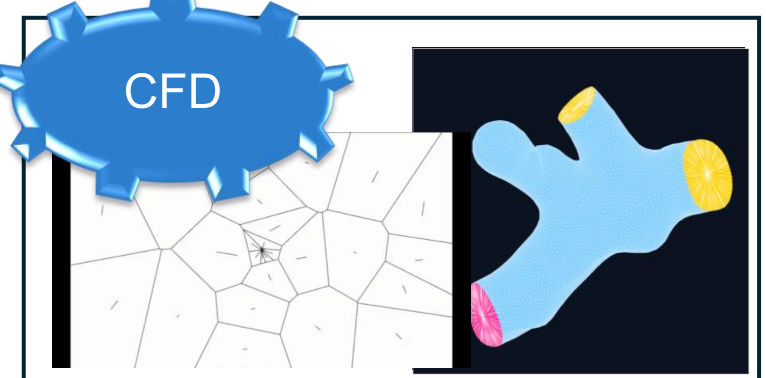

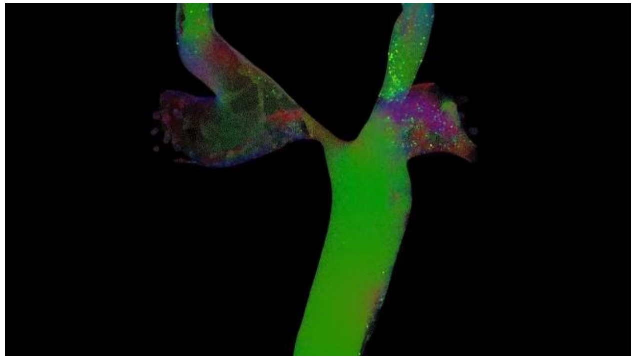

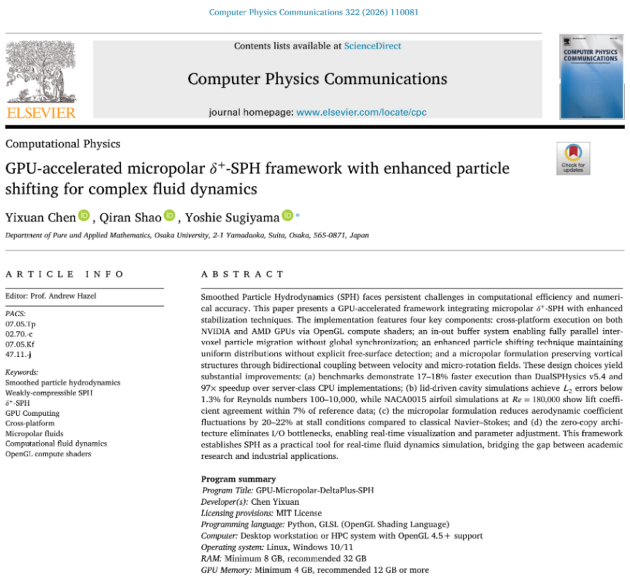

Computer Physics Communications 322 (2026) 110081

Contents lists available at ScienceDirect

Computer Physics Communications

journal homepage: www.elsevier.com/locate/cpc

ELSEVIER

Computational Physics

GPU-accelerated micropolar δ^{+}-SPH framework with enhanced particle shifting for complex fluid dynamics

Yixuan Chen, Qiran Shao, Yoshie Sugiyama *

Department of Pure and Applied Mathematics, Osaka University, 2-1 Yamadaoka, Suita, Osaka, 565-0871, Japan

A R T I C L E I N F O

Editor: Prof. Andrew Hazel

PACS:
07.05.Tp
02.70.-c
07.05.Kf
47.11.-j

Keywords:
Smoothed particle hydrodynamics
Weakly-compressible SPH
δ^{+}-SPH
GPU Computing
Cross-platform
Micropolar fluids
Computational fluid dynamics
OpenGL compute shaders

A B S T R A C T

Smoothed Particle Hydrodynamics (SPH) faces persistent challenges in computational efficiency and numerical accuracy. This paper presents a GPU-accelerated framework integrating micropolar δ^{+}-SPH with enhanced stabilization techniques. The implementation features four key components: cross-platform execution on both NVIDIA and AMD GPUs via OpenGL compute shaders; an in-out buffer system enabling fully parallel inter-voxel particle migration without global synchronization; an enhanced particle shifting technique maintaining uniform distributions without explicit free-surface detection; and a micropolar formulation preserving vortical structures through bidirectional coupling between velocity and micro-rotation fields. These design choices yield substantial improvements: (a) benchmarks demonstrate 17–18% faster execution than DualSPHysics v5.4 and 97× speedup over server-class CPU implementations; (b) lid-driven cavity simulations achieve L_2 errors below 1.3% for Reynolds numbers 100–10,000, while NACA0015 airfoil simulations at $Re = 180{,}000$ show lift coefficient agreement within 7% of reference data; (c) the micropolar formulation reduces aerodynamic coefficient fluctuations by 20–22% at stall conditions compared to classical Navier–Stokes; and (d) the zero-copy architecture eliminates I/O bottlenecks, enabling real-time visualization and parameter adjustment. This framework establishes SPH as a practical tool for real-time fluid dynamics simulation, bridging the gap between academic research and industrial applications.

Program summary
Program Title: GPU-Micropolar-DeltaPlus-SPH
Developer(s): Chen Yixuan
Licensing provisions: MIT License
Programming language: Python, GLSL (OpenGL Shading Language)
Computer: Desktop workstation or HPC system with OpenGL 4.5+ support
Operating system: Linux, Windows 10/11
RAM: Minimum 8 GB, recommended 32 GB
GPU Memory: Minimum 4 GB, recommended 12 GB or more

CREST

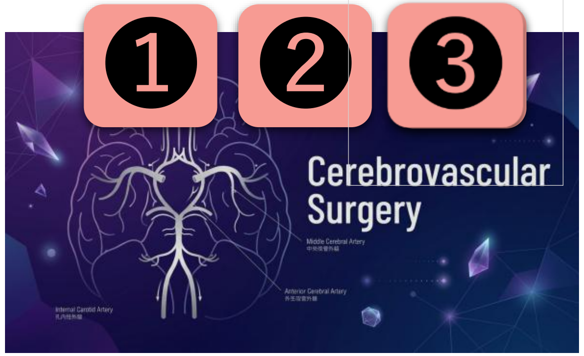

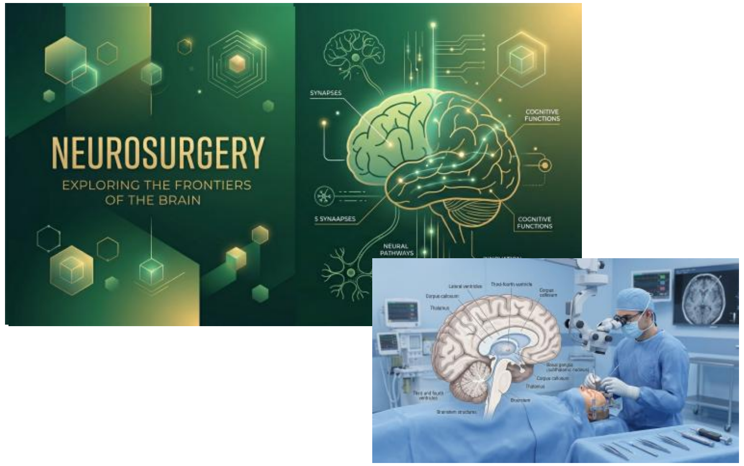

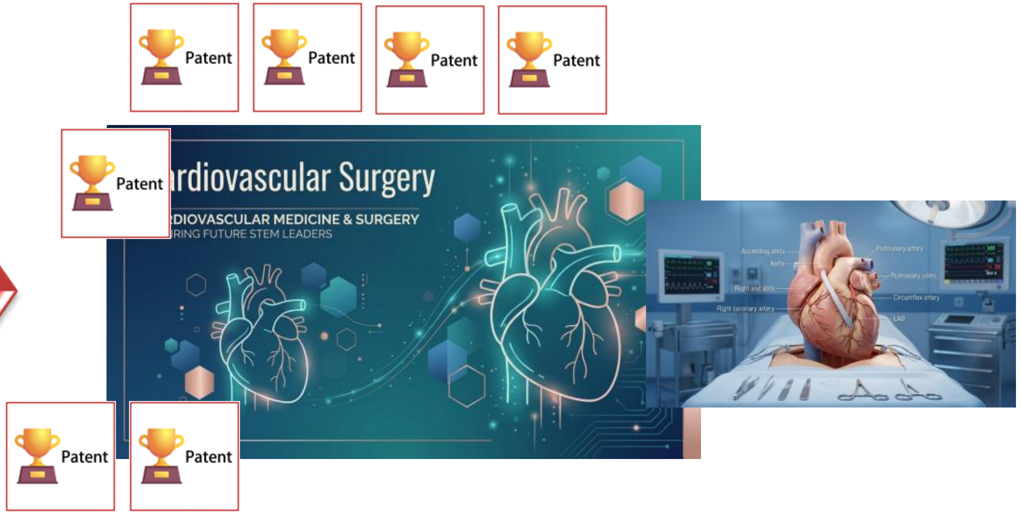

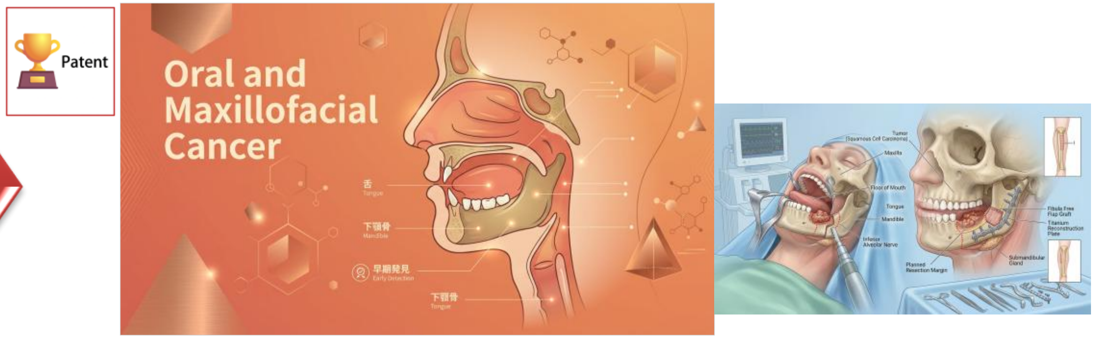

interdisciplinary research

Mathematics × Medicine × Information Science

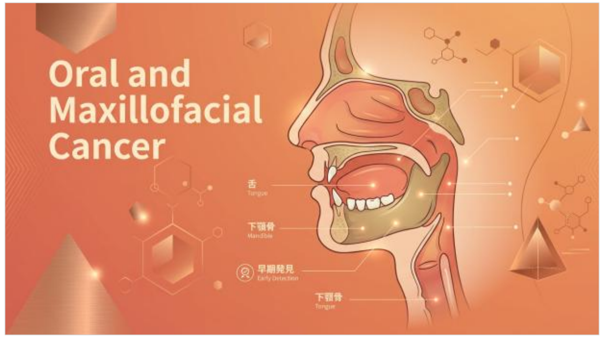

特許

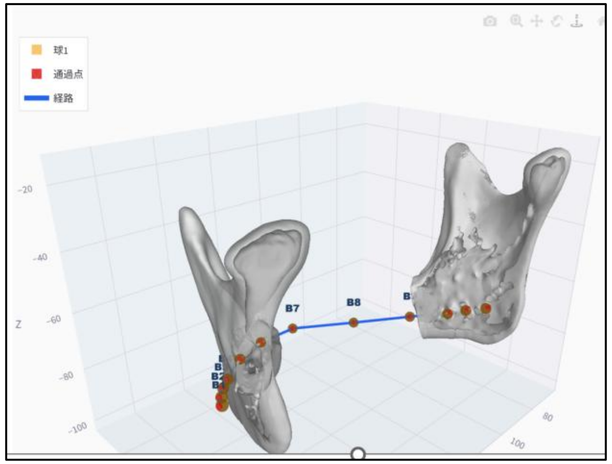

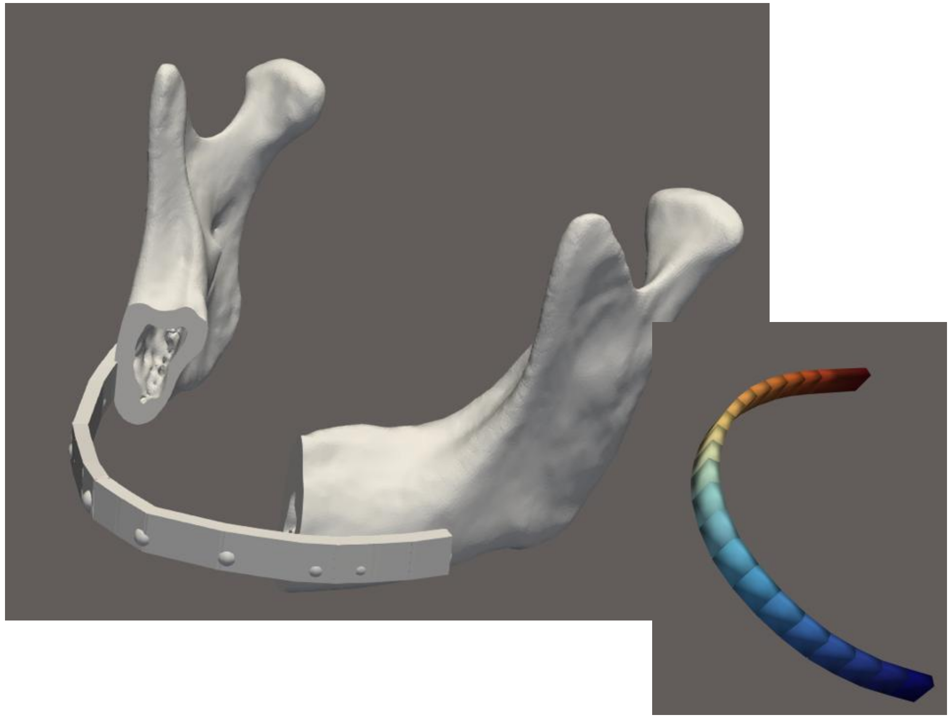

OSAKA UNIVERSITY

INTRO | MATH FOUNDATION | CLINICAL APP | COMP & AI | SUMMARY | DETAILS

Mathematical Analysis of Moving Boundary Problems - Part 1

MATHEMATICAL THEORY

1 Keller-Segel System Formulation

Keller-Segel system

論文

Let $d \geq 2$, $0 < T < \infty$ and $\gamma > 0$.

For $t \in (0, T]$, let $\Omega_t \subset \mathbb{R}^d$ be a bounded domain with $\partial\Omega_t \in C^2$ and set $Q_T := \bigcup_{0<t\leq T} \Omega_t \times \{t\}$.

(KS)
$$\begin{cases} \partial_t u = \Delta u - \nabla \cdot (u \nabla v) & \text{in } Q_T \\ 0 = \Delta v \ldots & \text{in } Q_T \\ & \text{on } \bigcup_{0<t<T} \partial\Omega_t \times \{t\} \\ & \text{in } \Omega_0 \end{cases}$$

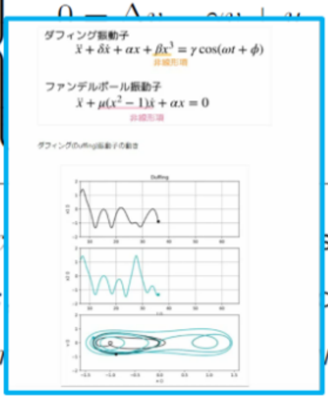

$$M\ddot{q} + Kq + \alpha q^3 = F(t)$$

- $u = u(x$ … si…
- $v = v(x$ … concentration of chemical attractant
- $n_t = {}^T($ … ward normal on $\partial\Omega_t$

4 / 15

2 Theorem: Well-posedness for (KS)

Main theorem

(KS)
$$\begin{cases} \partial_t u = \Delta u - \nabla \cdot (u \nabla v) & \text{in } Q_T \\ 0 = \Delta v - \gamma v + u & \text{in } Q_T \\ \partial_{n_t} u = \partial_{n_t} v = 0 & \text{on } \bigcup_{0<t<T} \partial\Omega_t \times \{t\} \\ u|_{t=0} = u_0 & \text{in } \Omega_0 \end{cases}$$

Theorem 2 (Local wlell-posedness for (KS))

Let $\tilde{u}$ be an unique strong solution of (CP) on $[0, T_*]$ obtained in Theorem 1.

For $(x, t) \in \overline{Q_{T_*}}$, we set functions u and v as

$$\begin{cases} u(x,t) := \tilde{u}(\varphi_t^{-1}(x), t), \\ v(x,t) := \tilde{v}(\varphi_t^{-1}(x), t). \end{cases}$$

Then (u, v) is an unique strong solution to (KS) such that

$$u(t),\ v(t) \in \mathcal{D}(\Delta_{\Omega_t}), \qquad t \in [0, T_*],$$

where Δ_{Ω_t} denotes the Neumann laplacian on Ω_t.

OSAKA UNIVERSITY

Thank You for Your Attention

AOWM - IPMU Workshop

March 6, 2026 · Kavli IPMU

Math × Med

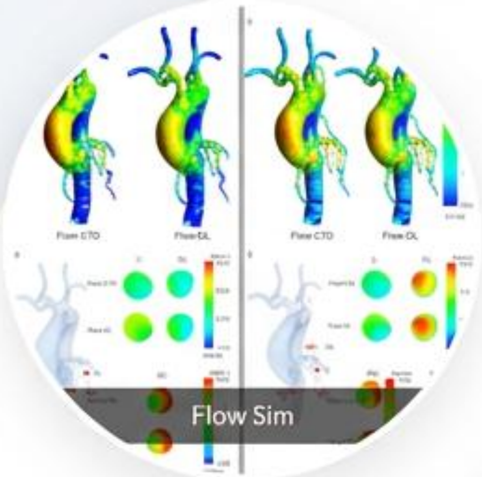

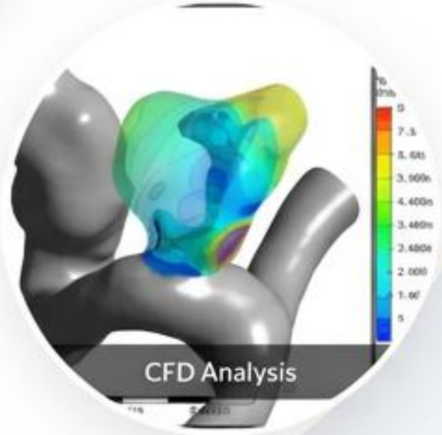

$$\nabla \cdot v = 0$$

HEMODYNAMICS · CFD ANALYSIS · AI INTEGRATION